Submission to *Ecosystems* (Revised manuscript)

Article type: Research Article

Title: Whole-ecosystem warming increases plant-available nitrogen and phosphorus in an ombrotrophic bog

Running title: Warming increases bog nutrient availability

List of Authors:

Colleen M. Iversen[1,2*] | John Latimer[3] | Deanne J. Brice[1,2] | Joanne Childs[1,2] | Holly M. Vander Stel[4] | Camille E. Defrenne[5] | Jake Graham[6] | Natalie A. Griffiths[1,2] | Avni Malhotra[7] | Richard J. Norby[8] | Keith C. Oleheiser[1,2] | Jana R. Phillips[1,2] | Verity G. Salmon[1,2] | Stephen D. Sebestyen[9] | Xiaojuan Yang[1,2] | Paul J. Hanson[1,2]

Institutional affiliations:

[1]Environmental Sciences Division, Oak Ridge National Laboratory, Oak Ridge, TN, USA;
[2]Climate Change Science Institute, Oak Ridge National Laboratory, Oak Ridge, TN, USA;
[3]XCEL Engineering, Oak Ridge, TN, USA;
[4]Kellogg Biological Station, Michigan State University, Hickory Corners, MI, USA;
[5]College of Forest Resources and Environmental Science, Michigan Technological University, Houghton, MI, USA;
[6]School of Civil & Environmental Engineering, Boise State University, Boise, Idaho, USA;
[7]Department of Geography, University of Zurich, Switzerland;
[8]University of Tennessee, Knoxville, TN, USA;
[9]Northern Research Station, USDA Forest Service, Grand Rapids, MN, USA

Contact Information:

Colleen M. Iversen, Environmental Sciences Division and Climate Change Science Institute, Oak Ridge National Laboratory, Oak Ridge, Tennessee, United States
Email: iversencm@ornl.gov
Telephone: (865) 332 – 8816

DR. COLLEEN M. IVERSEN (Orcid ID: 0000-0001-8293-3450)
JOHN LATIMER (No Orcid ID)
DEANNE J. BRICE (No Orcid ID)
JOANNE CHILDS (Orcid ID: 0000-0002-2002-7337)
HOLLY M. VANDER STEL (Orcid ID: 0000-0003-0077-3858)
DR. CAMILLE E. DEFRENNE (Orcid ID: 0000-0003-2767-4892)
DR. JAKE GRAHAM (No Orcid ID)
DR. NATALIE A. GRIFFITHS (Orcid ID: 0000-0003-0068-7714)
DR. AVNI MALHOTRA (Orcid ID: 0000-0002-7850-6402)
DR. RICHARD J. NORBY (Orcid ID: 0000-0002-0238-9828)
KEITH C. OLEHIESER (Orcid ID: 0000-0002-0875-2720)
JANA R. PHILLIPS (Orcid ID: 0000-0001-9319-2336)
DR. VERITY G. SALMON (Orcid ID: 0000-0002-2188-551X)
DR. STEPHEN D. SEBESTYEN (Orcid ID: 0000-0002-6315-0108)
DR. XIAOJUAN YANG (Orcid ID: 0000-0002-2686-745X)
DR. PAUL J. HANSON (Orcid ID: 0000-0001-7293-3561)

Funding information

United States Department of Energy, Office of Science, Biological and Environmental Research program

*This manuscript has been authored in part by UT-Battelle, LLC, under contract DE-AC05-00OR22725 with the US Department of Energy (DOE). The publisher acknowledges the US government license to provide public access under the DOE Public Access Plan (*http://energy.gov/downloads/doe-public-access-plan*).*

Author contributions

CMI designed and implemented the ion-exchange resin study, analyzed the data, and wrote the manuscript; JL collected, cleaned, and replaced ion-exchange resins from SPRUCE experimental enclosures; DB, JC, JP, and HVS extracted analyzed ion-exchange resin capsules and/or analyzed extracts for NH_4-N, NO_3-N, and PO_4-P; NAG, SDS, and KCO designed and implemented the porewater study, and KCO collected porewater and analyzed for nutrient concentrations; AM and JG collected information on resin elevation and depth to water table level; RJN and JC collected data on *Sphagnum* N and P requirement; VGS and CED assisted with the statistical framework and contextualization of available nutrients with plant-nutrient dynamics; XY ran the ELM-SPRUCE model to assess nutrient dynamics; PJH oversees and implements the SPRUCE experimental treatments, as well as the environmental data, above- and belowground. All co-authors read and commented on previous versions of the manuscript.

Data Archiving

Data presented in this manuscript have been appended to:

Iversen CM, Latimer J, Burnham A, Brice DJ, Childs J, Vander Stel HM. 2017. SPRUCE plant-available nutrients assessed with ion-exchange resins in experimental plots, beginning in 2013. Carbon Dioxide Information Analysis Center, Oak Ridge National Laboratory, U.S. Department of Energy, Oak Ridge, Tennessee, U.S.A. Data set accessed at http://dx.doi.org/10.3334/CDIAC/spruce.036.

Abstract

Warming is expected to increase the net release of carbon from peatland soils, contributing to future warming. This positive feedback may be moderated by the response of peatland vegetation to rising atmospheric [CO_2] or to increased soil nutrient availability. We asked whether a gradient of whole-ecosystem warming (from +0°C to +9°C) would increase plant-available nitrogen and phosphorus in an ombrotrophic bog in northern Minnesota, USA, and whether elevated [CO_2] would modify the nutrient response. We tracked changes in plant-available nutrients across space and through time and in comparison with other nutrient pools, and assessed whether nutrient warming responses were captured by a point version of the land-surface model, ELM-SPRUCE. We found that warming exponentially increased plant-available ammonium and phosphate, but that nutrient dynamics were unaffected by elevated [CO_2]. The warming response increased by an order of magnitude between the first and fourth year of the experimental manipulation, perhaps because of dramatic mortality of *Sphagnum* mosses in the surface peat of the warmest treatments. However, neither the magnitude nor the temporal dynamics of the responses were captured by ELM-SPRUCE. Relative increases in plant-available ammonium and phosphate with warming were similar, but the response varied across raised hummocks and depressed hollows and with peat depth. Plant-available nutrient dynamics were only loosely correlated with inorganic and organic porewater nutrients, likely representing different processes. Future predictions of peatland nutrient availability under climate change scenarios must account for dynamic changes in nutrient acquisition by plants and microbes, as well as microtopography and peat depth.

Keywords

warming, elevated [CO_2], nutrient availability, ombrotrophic bog, SPRUCE, peat depth, microtopography, *Sphagnum* moss, nitrogen, phosphorus

Highlights:

- We investigated the nutrient dynamics underpinning peatland responses to changing environmental conditions within the framework of a large-scale warming × CO_2-enrichment experiment in a nutrient-limited ombrotrophic bog at the southern end of the boreal peatland range. Whole-ecosystem warming exponentially increased plant-available ammonium and phosphate, but nutrient dynamics were unaffected by elevated [CO_2].
- The nutrient warming response increased by an order of magnitude between the first and fourth years of warming, perhaps because of dramatic mortality of *Sphagnum* mosses in the surface peat of the warmest treatments. However, this response was not captured by a land surface model parameterized to simulate ecosystem dynamics within the experiment.
- Relative increases in plant-available ammonium and phosphate with warming were similar, but the warming response varied across raised hummocks and depressed hollows and with peat depth.

Introduction

Peatlands store at least one-third of global soil organic carbon (C) in deep deposits of peat accumulated over millennia due to an imbalance between production and decomposition (Bridgham and others 2006; Gorham, 1991; Nichols and others 2019). Warming is expected to increase the net release of C from peatland soils, potentially leading to a positive feedback to future warming (Bridgham and others 2008), though these responses could be moderated by elevated [CO_2] or increased peat nutrient availability (Hedwall and others 2017; Milla and others 2006; van der Heijden and others 2000). Here we investigated the nutrient dynamics underpinning peatland responses to changing environmental conditions within the framework of a large-scale warming × CO_2-enrichment experiment in a nutrient-limited ombrotrophic bog at the southern end of the boreal peatland range (i.e., the Spruce and Peatland Responses Under Changing Environments, or 'SPRUCE' experiment; Hanson and others 2017).

Warming has been shown to increase nutrient mineralization rates across a range of upland ecosystems (Rustad and others 2001), and in ecosystems underlain by organic soil (Aerts and others 2006; Munir and others 2017; Salazar and others 2020; Weedon and others 2012). Increased nutrient availability has been found to increase (Bragazza and others 2006; Mack and others 2004) or inhibit (Keller and others 2006; Malhotra and others 2018; Olid and others 2014) peat decomposition rates due to complex interactions among microbial physiology, plant species composition and litter chemistry, and edaphic conditions. Increasing nutrient availability can also change the balance among the fractional cover and biomass of vascular overstory plants and *Sphagnum* mosses, as *Sphagnum* is less competitive at higher levels of nutrient availability (Berendse and others 2001; Vitt and others 1990). Microbial and vegetation responses to

increased nutrient availability could be moderated by potential declines in soil moisture and water table levels associated with warming (Weltzin and others 2003).

Nitrogen (N) and phosphorus (P) have different rates of mineralization and immobilization, which are controlled by differing microbial communities, plant-rhizosphere interactions, and edaphic and environmental factors (Richardson and others 2009; Spohn and others 2013; Vitousek and others 1991; Walker and others 1976). Nitrogen and P cycling rates and have been shown to respond differently to warming in boreal peatlands (Munir and others 2017) and to freeze-thaw or heatwave events in uplands (Mooshammer and others 2017), with potential implications for shifting plant and microbial communities (Hill and others 2014; Iversen and others 2010; Koerselman and others 1996; Wang and others 2014).

Peatlands are also characterized by small-scale environmental gradients – from undulating surface microtopography, which encompasses raised hummocks and depressed hollows within the span of 1 m (Eppinga and others 2010) – to changes in peat and porewater characteristics, soil moisture and oxygenation, and microbial community abundance and composition with peat depth (Griffiths and others 2017; Griffiths & Sebestyen, 2016; Griffiths and others 2019; Tfaily and others 2018; Wang and others 2015; Wilson and others 2021a,b). Microtopographic positions have been shown to have different nutrient availabilities under ambient conditions (Eppinga and others 2010) and to respond differently to small-scale experimental warming (Munir and others 2017). However, how nutrient availability will change with depth throughout the peat profile in response to warming remains an open question, as prior investigations of nutrient response to warming in peatlands have focused on surface peat (Munir and others 2017; Weedon and others 2012). Nutrient availability in ecosystems underlain by organic soils is generally greater within deep peat layers located beyond the reach of plant roots that are often

112 constrained to surface aerobic horizons (Iversen and others 2018; Keuper and others 2012;
113 Murphy and others 2010). Warming in peatlands could therefore lead to increased availability of
114 nutrients in the shallow rooting zone, and in turn, warming-induced drying could also allow roots
115 to access deeper nutrients.

116 Increases in global mean surface air temperature are projected to be as much as 3.3 to 5.7°C by
117 2100, following the rise in atmospheric carbon dioxide concentrations ($[CO_2]$) and other
118 greenhouse gases due to anthropogenic activities (IPCC, 2021). Thus any impacts of warming on
119 peatland nutrient cycling must be considered in the context of elevated $[CO_2]$, which might
120 stimulate plant growth and rhizosphere C availability (Walker and others 2021), potentially
121 leading to increased nutrient immobilization in vegetation and microbial communities (de Graaff
122 and others 2006; Finzi and others 2007). However, evidence for changes in ecosystem C and
123 nutrient cycling in response to elevated $[CO_2]$ is generally based on upland ecosystems (but see
124 Berendse and others 2001; Fenner and others 2007; Milla and others 2006; Toet and others 2006;
125 van der Heijden and others 2000).

126 Terrestrial biosphere models are a tool that can be used to encode hypotheses about ecosystem
127 responses to changing environmental conditions but must be compared with and validated
128 against observations of changes in ecosystem C and nutrient cycling in response to a range of
129 possible futures (Medlyn and others 2015). ELM-SPRUCE, a point version of the land
130 component of the Energy Exascale Earth System Model (E3SM), has been specifically designed
131 to simulate ecosystem responses to warming and elevated $[CO_2]$ at SPRUCE. ELM-SPRUCE
132 includes coupled C, N and P cycle dynamics (Burrows and others 2020; Yang and others 2019)
133 as well as ombrotrophic bog hydrology, hummock and hollow microtopography, and *Sphagnum*

134 moss as a unique plant functional type (Griffiths and others 2017; Shi and others 2021; Shi and
135 others 2015).

136 Here we asked whether a gradient of whole-ecosystem warming would increase plant-available
137 nitrogen and phosphorus in an ombrotrophic bog in northern Minnesota, USA, and whether
138 elevated [CO_2] would modify the nutrient response. We further considered whether nutrient
139 responses to warming varied across space and through time, focusing in particular on the rooting
140 zone (and the surface zone where non-vascular mosses have access to nutrients). We used ion-
141 exchange resins to assess inorganic plant-available nutrients across hummock-hollow
142 microtopography and throughout the peat profile at monthly and cumulative annual time steps
143 (and henceforth refer to these fluxes as 'resin-available nutrients'). Because bogs are unique
144 ecosystems where vegetation has access to near-surface porewater as a potential source of
145 nutrients, we also compared responses inferred from ion-exchange resins to the dynamics of
146 inorganic and organic nutrients observed in porewater. We compared observed resin-available
147 nutrient dynamics to ELM-SPRUCE model predictions of net nutrient mineralization in the
148 SPRUCE experiment.

149 **Materials and Methods**

150 ***The SPRUCE experiment***

151 The Spruce and Peatland Responses Under Changing Environments (SPRUCE) experiment is
152 located in the ombrotrophic S1 Bog on the Marcell Experimental Forest in northern Minnesota,
153 USA (47°30.476' N; 93°27.162' W; 418 m above mean sea level; Sebestyen and others 2011).
154 SPRUCE is located at the southern end of the range of boreal peatlands and is therefore expected
155 to be especially vulnerable to warming conditions. The S1 Bog, similar to other bog basins in the
156 area and region, has accumulated from 2 m to 11 m of C-rich peat over the last 11,000 years

(McFarlane and others 2018; Parsekian and others 2012). The overstory is dominated by the trees *Picea mariana* (black spruce) and *Larix laricina* (larch), with an understory dominated by ericaceous shrubs (McPartland and others 2020). The bog surface is carpeted by *Sphagnum* mosses, with a minor presence of other mosses (for more information on mosses within the SPRUCE experiment, see Norby and others 2019). The effects of above- and belowground warming and elevated [CO_2] on peatland processes are being assessed in 12.8-m wide by 7-m tall enclosures underlain by belowground corrals (see Figure 1 for enclosure layout and description of treatments and see Hanson and others (2017) and Sebestyen & Griffiths (2016, data citation) for more details). The SPRUCE experimental design is regression-based; two series of five enclosures are warmed at set point levels of either +0°C, +2.25°C, +4.5°C, +6.75°C, or +9°C above ambient conditions. Aboveground warming is accomplished by introducing warm air generated from propane-fired heat exchangers into the enclosures via forced-air heating distributed around the base of the enclosure. Half of the enclosures also receive elevated [CO_2] via the injection of pure CO_2 into the air circulation ducts to attain a target level of +500 ppm to replicate conditions predicted for the end of the 21st century (Hanson and others 2017). SPRUCE is unique in that it exposes large experimental enclosures to 'whole-ecosystem' warming; belowground warming is accomplished with 3-m deep heating rods that encircle and intersperse each enclosure. The encircling heating rods provide heat from 0-3 m depth, while rods within the enclosures only heat from 2-3 m depth to avoid hot spots of direct heating within the rooting zone. This system provides a uniformly warmed volume of peat belowground (Barbier and others 2013).

Beneath each enclosure, the belowground peat volume is encircled by a corral constructed from interlocking piles that reach beneath the peat horizons to the subtending mineral soils. The corral

isolates the biogeochemical and hydrological system associated with each enclosure so that each enclosure can be conceptualized as a 'miniature bog' exposed to a future climate. The belowground corrals also allow quantification of outflow, the shallow lateral flow analogous to runoff via natural passive drainage (data citation: Sebestyen & Griffiths 2016). SPRUCE treatments began with deep-peat warming in 2014 and installation of the corrals in winter 2014 – 2015; aboveground warming began in August 2015, and elevated [CO_2] additions began in early June 2016 during the first full year of whole-ecosystem warming (Hanson and others 2017).

Although the SPRUCE treatments are applied as differential levels of warming and CO_2 additions, because biological systems respond to actual temperatures we express and evaluate nutrient responses to warming by comparisons to measured peat temperatures at the depth of resin incubations rather than the nominal temperature treatments.

Plant-available nutrients assessed using ion-exchange resins

Plant-available nutrients were assessed using mixed-bed ion-exchange resin capsules (i.e., containing both anion, OH-, and cation, H+, resins). Ion-exchange resins have been shown to accurately integrate and represent plant-available ammonium (NH_4-N) and phosphate (PO_4-P) across space and through time, including in ecosystems underlain by organic soils (Bridgham and others 2001; Giblin and others 1994; Gu and others 2020), and have been tested at soil temperatures up to 30°C (Yang and others 1991). The resin capsules at SPRUCE were inserted, incubated, and extracted serially beginning in 2013 and the collections are on-going (data citation: Iversen and others 2017). Data presented here span the full years of 2014 to 2018 and therefore include periods of belowground warming only (2014), above- and belowground warming (2015) and above- and belowground warming with elevated [CO_2] (2016-2018). PVC resin-access tubes (Wecsa, Inc., LLC) allowed removal and replacement of the resin capsule

without disturbing the peat profile. Access tubes consisted of a 3.2-cm diameter outer tube with a 1.9-cm diameter inner access tube with a resin capsule attached to the base (see Figure S1; as in Iversen and others 2018). Resin-access tubes were installed in June 2013 at a 30° angle from vertical across hummock and hollow microtopography and throughout the shallow peat profile to a depth of 60 cm in hummocks and 30 cm in hollows. Hummock-hollow access-tube arrays were installed in two locations in each of the ten SPRUCE experimental enclosures, as well as two locations in each of two ambient, unenclosed plots (Figure 1).

Locations and elevations of each access-tube array were estimated by terrestrial laser scanning (TLS) using a Riegl VZ-1000 terrestrial laser scanner (Riegl Laser Measurement Systems, Riegl USA, Inc., Winter Garden, FL, USA) as in Graham and others (2020). Briefly, 50-cm tall dowels that had reflectors on their tops were inserted at the peat surface in May 2018, before the TLS scan. The location of the dowel was optimized to reflect the average elevation of the resin-access tube arrays. Elevation was then calculated by subtracting 50 cm. On average, hummocks were ~15 cm higher in elevation than adjacent hollows, with a few exceptions (Table S1).

UNIBEST resin capsules (UNIBEST, Inc., Walla Walla, WA, USA) were placed into contact with the soil at the base of the inner resin-access tube (11.4 cm^2 of the rounded capsule surface protruded from the base of the tube; Figure S1f) and incubated *in situ* for approximately 28 days before collection and replacement with a new resin capsule. In cases where resins were frozen into the bog during winter months and unable to be removed, we assumed that the unfrozen time-period was no longer than 28 days (we refer to this collection timeframe as *monthly* below, to differentiate from *annual* nutrient availability). Peat was cleaned from the removed capsules by rinsing with distilled water, and the capsules were air-dried prior to shipment to Oak Ridge National Laboratory (ORNL). At ORNL, the air-dried capsules were serially extracted with 2 M

potassium chloride, and the extractant was frozen at -20ºC until analysis for nutrient concentrations on a Lachat QuikChem 8500 flow injection analysis autoanalyzer (Hach Company, Loveland, CO, USA) as in Iversen and others (2017, data citation). Nutrient adsorption was blank-corrected based on unincubated resins, standardized per unit of resin capsule surface area, and either standardized per 28 days or summed over a calendar year as a cumulative annual total. Previous studies with these resin capsules indicate they continue to accumulate nutrients over time without saturation (Skogley and others 1996; Yang and others 1991). In the few cases where an observation was lost during sampling or processing, the value from the second resin array in the same enclosure, at the same microtopographic position and peat depth, was substituted to derive annual cumulative totals. Given that NO_3-N adsorbed to resins was negligible and often below detection limits (as might be expected in a saturated, acidic bog ecosystem, Bridgham and others 2001), we focus on resin-available NH_4-N and PO_4-P for the purposes of this paper.

Resins mimic a plant root, exchanging ions with the surrounding soil system, allowing us to quantify the *in situ* availability of nutrients for plant acquisition. However, we note that resin-accumulated nutrients are the balance of production (gross nutrient mineralization) and consumption (nutrient immobilization) by surrounding plants, microbes, and soil surfaces. While this is similar to the competitive environment experienced by plant roots, these competing processes must be kept in mind when interpreting observed patterns in resin-available nutrient dynamics. We further compared responses inferred from ion-exchange resins to the dynamics of inorganic nutrients observed in porewater because vegetation has access to near-surface porewater as a potential source of nutrients and porewater is frequently measured across saturated peatland ecosystems (Bourbonniere 2009).

249 We focused on inorganic nutrient availability given that we were able to capture its accumulation
250 over time and with peat depth using non-destructive ion-exchange resin sampling. However,
251 vegetation in boreal systems has been shown to acquire organic nutrients (Kielland and others
252 2006), so we also compared the patterns observed in resin-available nutrients to organic nutrients
253 in porewater to gain a broader view of plant-available N and P.

254 ***Porewater nutrients***

255 A nest of six depth-specific (10-cm screened sections) piezometers per enclosure allowed
256 collection of porewater throughout the peat profile (0-3 m) in hollow microtopography. Water
257 samples were collected every 2 weeks using a peristaltic pump and analyzed for nutrients (NH_4-
258 N, NO_3-N, and soluble reactive phosphorus, SRP), as well as total N (TN) and total P (TP) at the
259 United States Forest Service laboratory in Grand Rapids, MN, USA. Soluble reactive P
260 concentration (SRP) is largely equivalent to phosphate concentration (PO_4^{3-}) in water, though
261 some condensed phosphate may be measured along with orthophosphate in the colorimetric
262 method that we used to determine SRP (APHA, 2017). Ammonium, NO_3-N, SRP, TN, and TP
263 concentrations were quantified via analysis on a Lachat QuikChem autoanalyzer as described in
264 Griffiths and others (2016b, data citation). We focused on the porewater nutrient concentrations
265 at 0-10 cm and 30-40 cm depths to facilitate direct comparison with ion-exchange resins
266 incubated at those depths in adjacent hollows. We averaged the nutrient concentrations for
267 porewater samples that were collected within the dates of the approximately monthly resin
268 incubations, beginning in 2015 and extending through 2018. We calculated 'organic N' and
269 'organic P' as the difference between total N and inorganic N and total P and inorganic P,
270 respectively (where organic N was equal to '0' if the difference resulted in a slightly negative
271 number). When porewater nutrients were below detection limits, we used half the detection value

as the value for that collection date (the detection limit varied according to methodology described in data citation: Griffiths and others 2016b).

Potential nutrient competition

In order to understand the surface dynamics of resin-available nutrients over time, we compared patterns in resin-available NH_4-N and PO_4-P to patterns in the nutrient requirements of *Sphagnum* mosses given its mortality in response to warming at SPRUCE in later treatment years (Norby and others 2019). *Sphagnum* nutrient requirement was calculated using growth and N and P concentration estimates from each of the dominant *Sphagnum* species measured annually in October 2016, 2017, and 2018 in each experimental enclosure (methods described in Norby and others 2019, and data citations: Norby and others 2018 and 2020). The enclosure-scale N or P requirement for new growth is the concentration of the element in species-specific new growth times the dry matter increment, scaled by fractional cover of each *Sphagnum* species (g N/m^2 or g P/m^2).

While mineral surfaces can immobilize PO_4-P (Richardson, 1985), the peat in the S1 Bog where the SPRUCE experimental enclosures are located has limited mineral content to a depth of at least 2 m (data citation: Iversen and others 2014). The S1 Bog also has limited bulk and extractable Al and Fe content throughout (Herndon and others 2019; Tfaily and others 2014), though the relationship between P and Fe in surface peat appears to be increasing with warming (Curtinrich and others 2021).

Edaphic and environmental conditions in the SPRUCE enclosures

Peat temperature. We investigated the temperature response of resin-available nutrients, both during the 28-day periods of resin deployment and over the course of each year, using peat

294 temperature measurements collected from multipoint thermistor probes (W.H. Cooke & Co. Inc,
295 Hanover, PA, USA). The probes were installed in each SPRUCE experimental enclosure in 2014
296 in zone B (i.e., the zone in the middle of the SPRUCE experimental enclosures; for more
297 information about probe locations, installation, and calibration, see data citation: Hanson and
298 others 2016). The depth of interest for each soil temperature probe was chosen to most closely
299 match the targeted incubation depth of ion-exchange resin capsules (i.e., probes installed in
300 hummocks at ~20 cm and ~ 0 cm above the hollow surface, and probes installed in hollows at
301 ~10 cm and ~30 cm below hollow surface; see Table S2).

302 *Water table.* Automated water table elevation measurements and normalization for each
303 enclosure with respect to hollow heights are explained in detail in Hanson and others (2020b,
304 data citation). Briefly, water table elevation measurements collected beginning in 2015 were
305 obtained in stainless steel well casings (Drillers Services, Inc.) centered within each SPRUCE
306 enclosure. The water height within each well was measured with automated sensors (Model WT-
307 VO 2000; TruTrack, Christchurch, New Zealand). Water table absolute elevations in meters
308 were referenced to surveyed elevations of the tops of all wells (data citation: Griffiths and others
309 2016a), and water level with respect to the mean hollow elevation of an enclosure were
310 normalized to the water height in the well during a uniform post-rainfall, post-drainage period
311 when water tables were just at or below the peat hollows. We only include a water table
312 comparison when the average peat temperature at the depth of each incubated resin was above
313 0°C for each incubation period.

314 ***Simulated nutrient availability responses to warming using ELM-SPRUCE***

315 We used ELM-SPRUCE, a version of the Energy Exascale Earth System Model (E3SM) land
316 model (version 1, ELM v1), to simulate nutrient responses to warming and elevated [CO_2] at

SPRUCE. Building on the Community Land Model version 4.5 (CLM4.5), ELM v1 has undergone several major developments in recent years. These new developments include the coupling of C, N and P cycle dynamics, the introduction of dynamic storage pools for C, N and P, the improved representation of the effects of nutrient limitation on plant growth, improved phenology for deciduous forests, and various improvements in model parameterization (Burrows and others 2020; Yang and others 2019). Compared to ELM v1, ELM-SPRUCE includes additional processes and plant functional types that are specific to peatland ecosystems (Griffiths and others 2017; Shi and others 2021; Shi and others 2015). Observational data from the S1 Bog used for model parameterization included leaf- and fine-root N and P concentrations (Salmon and others 2021) and rooting depth for fine roots (Iversen and others 2018). Model evaluation using pretreatment observations of vegetation biomass, growth, and nutrient requirements suggests that ELM-SPRUCE is generally able to capture the observed C and nutrient pools and fluxes (Griffiths and others 2017; Salmon and others 2021).

Model simulations for the current study included three steps: (1) Model spin-up to generate pre-industrial steady-state for C, N and P pools in vegetation and soils, (2) Transient simulations from 1850-2014 in which historical atmospheric CO_2 concentrations and N deposition were used as driving data, and (3) Simulations of treatment responses between 2015-2018, in which treatment-specific air temperature and atmospheric CO_2 concentrations were used as driving data. In total, there were 11 simulations corresponding to 10 experimental treatments and 1 ambient plot at SPRUCE. We focused here on the outputs of annual cumulative net N and P mineralization from treatment simulations between 2016-2018. Net nutrient mineralization per unit peat volume is an imperfect comparison to annual resin-available nutrient accumulation but was the closest nutrient flux available from among the model outputs and integrates similar

processes of nutrient mineralization and immobilization (e.g., Bridgham and others 2001). Here we compare resin-available nutrients with ELM-SPRUCE simulated net nutrient mineralization responses in a qualitative way with the goal of identifying important gaps in model representation of nutrient cycle dynamics in peatland ecosystems. Gross nutrient mineralization in ELM-SPRUCE is modeled using a Q_{10} approach (where $Q_{10} = 1.5$) and resulting net nutrient mineralization is the remainder after microbial nutrient immobilization.

Statistical analyses

Resin-available nutrient responses to warming and elevated [CO_2]

We used R version 4.0.3 in our statistical analyses (R Core Team, 2021) to examine resin-available nutrient responses to warming and elevated [CO_2] in the SPRUCE experimental enclosures from 2014 to 2018. We do not include data from unenclosed, ambient plots in our statistical models (as in Hanson and others 2020a). However, ambient plots were measured to quantify potential experimental artifacts and the data are summarized in Table 1. Peat temperature and the availability of NH_4-N and PO_4-P differed somewhat between the +0°C enclosures and the unenclosed, ambient plots, though differences varied by peat depth and among plots (see *Supplementary Statistical Methods* and Table 1).

We assessed responses of resin-available nutrients to warming in the enclosures in two ways: first, we examined the variation in the cumulative annual availability of NH_4-N and PO_4-P, as well as the ratio of the two. We expected that the N/P ratio would provide an assessment of whether resin-available NH_4-N and PO_4-P differed in their response to warming, and also what the implications might be for vegetation N or P limitation (Koerselman & Arthur, 1996). To assess these *annual responses*, we compared several potential linear mixed-effect models to consider the effects of warming, elevated [CO_2], microtopography, peat depth, and year on

363 nutrient dynamics using the *lmer* function in the *lme4* package in R (see additional detail in
364 *Supplementary Statistical Methods*; Harrison and others 2018). In these models, both warming
365 and elevated [CO_2] were treated as fixed effects, where warming was a numerical vector of the
366 average annual peat temperature measured at the peat depth closest to that of the resin depth and
367 CO_2 was a discrete variable (e.g., 'ambient' or 'elevated'). Peat depth and microtopographic
368 position were combined into a discrete, fixed effect in the models called 'topodepth' (e.g.,
369 hummock at 10 cm, hummock at 30 cm, hollow at 10 cm, etc.). We assumed that year was an
370 important factor given the progression in SPRUCE treatment application, and year was treated as
371 a discrete, fixed effect in the models. In turn, we included enclosure as a random effect in the
372 models (with both a random intercept and a random slope) to account for random differences
373 among enclosures and repeated sampling of enclosures that were not explained by our fixed
374 effects. Cumulative annual resin-available nutrients and nutrient ratios were log-transformed
375 prior to statistical analyses to meet model assumptions. We selected a final model based on AIC
376 criteria, as well as standard model selection processes (see *Supplementary Statistical Methods* for
377 more information; Harrison and others 2018). We made pairwise comparisons by topodepth and
378 year using the *pairwise* function in the *emmeans* package in R (Table S3).

379 After considering the annual accumulation of resin-available nutrients, we examined the
380 variation in accumulated NH_4-N and PO_4-P over the ~28-day timeframe (i.e., the *monthly*
381 responses). Examining the monthly patterns in resin-available nutrients allowed us to consider
382 the additional factor of depth to the water table, which varied seasonally within a year and
383 therefore could not be analyzed on an annual basis. Given the correlation between peat
384 temperature and depth to water table, we used a principal components analysis to obtain a
385 continuous variable representing the combination of peat temperature and distance to water table

and used this variable in a new set of linear mixed-effects models (see details in *Supplementary Statistical Methods*). However, these monthly models were similar to the annual models, and further investigation showed that that water table level – which had not yet changed substantially in response to warming – had little power to explain (less than 10%) observed changes in resin-available nutrients (see *Supplementary Statistical Methods*, Figures WT1 and WT2). Thus we do not discuss water table results further here.

We did disentangle peat temperature from depth to water table to further explore the temperature sensitivity of monthly nutrient availability. We fit Q_{10} relationships to the monthly accumulation of resin-available nutrients at a given peat temperature (Lloyd and others 1994). Curves were fit in Sigma Plot (version 14.5, Systat Software, Inpixon HQ, USA) using the equation: Resin-Available Nutrient ($\mu g\ cm^{-2}\ 28\ days^{-1}$) = $R_{12} \times Q_{10}^{((\text{Peat Temperature}-12)/10)}$, where R_{12} is the baseline resin-available nutrient flux during incubation period (targeted at 28 days) at 12°C, a temperature near the midpoint of the range of peat temperatures across warming treatments, peat depths, and microtopographic positions. To obtain a warming response for model comparison, we fit Q_{10} relationships to observations from all enclosures at a given topodepth across all years as well as for the most recent observation year of 2018. For comparison, we also fit Q_{10} response functions to model projections of cumulative annual net N and P mineralization.

Comparisons among resin-available nutrients and other nutrient pools

We examined the relationship between *Sphagnum* annual N and P requirement (g nutrient m^{-2} $year^{-1}$) and surface resin-available NH_4-N and PO_4-P at 10-cm depth in hummocks and hollows using log-linear regressions. Furthermore, we examined whether resin-available nutrients were correlated with porewater inorganic, organic, and total nutrients. Given that log-transformation

408 did not result in normally-distributed data, we used a non-parametric correlation for the
409 porewater comparisons (Spearman's Rho; *stats* package in R).

410 **Results**

411 ***Cumulative annual resin-available nutrients increased with warming but varied with peat***
412 ***depth and microtopography***

413 NH_4-N was by far the most available N source, with NO_3-N making up a negligible fraction; PO_4
414 availability was intermediate between NH_4-N and NO_3-N. Warming increased cumulative annual
415 resin-available NH_4-N and PO_4-P, but the magnitude of the response varied across
416 microtopographic positions and with peat depth and increased over time. There were no
417 significant effects of elevated [CO_2] on resin-available nutrients (Table 1). Neither warming nor
418 elevated [CO_2] had a significant effect on the cumulative annual ratio of resin-available N/P,
419 though resin-available N/P ratio increased with peat depth (Table 1 and Table S3).

420 The best overall model fit to explain the variability in NH_4-N and PO_4-P and their ratio (i.e., the
421 model with the lowest AIC) included the average annual peat temperature at the depth closest to
422 that of the resin, as well as combined hummock-hollow microtopographic position and depth
423 (i.e., the 'topodepth' term), and year, with enclosure as a random factor (conditional R^2 = 0.77,
424 0.71, and 0.43 for NH_4-N, PO_4-P, and N/P ratio models, respectively; Figure 2). A model
425 including elevated [CO_2] did not provide a better fit to any of the resin-available nutrient data
426 (See *Supplementary Statistical Methods*). Within the best-fit model for NH_4-N and PO_4-P, we
427 also observed significant interactions between warming and topodepth, as well as warming and
428 year, and we observed an increase in the strength of the warming × year interaction over time
429 (Figure 2, *Supplementary Statistical Methods*). In turn, the best-fit linear mixed-effect model for

cumulative annual N/P ratio also included a significant interaction between topodepth and year (Figure S2, *Supplementary Statistical Methods*).

Given the significant interactions with warming, we also fit separate log-linear models to average annual peat temperature at a given topodepth and log-transformed cumulative available NH_4-N, PO_4-P, and the ratio of the two at each microtopographic position and peat depth, across all years (Figure 3) and within a single year (Table S4). The only significant log-linear models between peat temperature and resin-available NH_4-N or PO_4-P indicated an exponential increase in resin-available nutrients with increasing peat temperature at deeper peat depths (Figure 3) and in more recent years (Table S4). We saw no significant relationships between annual N/P ratio and warming at any topodepth position either within or across years (Table S4, with the exception of an extremely weak relationship at 60-cm peat depth).

Within a given treatment year, resin-available NH_4-N and PO_4-P tended to be least in shallow peat and less in raised hummocks compared with depressed hollows (Tables 1 and S3, Figure 3). Averaged across all enclosures, resin-available NH_4-N to PO_4-P were significantly greater in 2018 than in previous years (Figure 2; Table S3). In turn, the ratio of cumulative annual available NH_4-N to PO_4-P ranged from ~1:1 to 175:1 across all years, microtopographic positions, and peat depths (Table 1).

ELM-SPRUCE predicted increases in annual net nutrient mineralization with warming

Across all topodepths, ELM-SPRUCE predicted increases in annual cumulative net N and P mineralization with warming (Figure 4), but the magnitudes of the warming responses in model simulations (assessed by Q_{10} response functions) were much lower than the warming responses observed in the resin-available nutrient data, especially in surface soils (Table S5). As with observed resin-available nutrient dynamics (Table 1), model prediction of net N and P

453 mineralization was greater in the hollows than in the hummocks, but in contrast to the
454 observations, model-predicted net nutrient mineralization tended to decrease with peat depth
455 (Figure 4).

456 ***Large increases in shallow peat resin-available nutrients were correlated with mortality of***
457 ***Sphagnum mosses in warmest enclosures***

458 The increase in cumulative annual resin-available nutrients with warming had initially been
459 much greater below the rooting zone (i.e., at 60- and 30-cm depths in hummocks and hollows,
460 respectively, Table 1, Figures 2, 3), but this changed in later treatment years, where we saw large
461 increases in both NH_4-N and PO_4-P at 10-cm peat depth in both hummocks and hollows (Table
462 1, Figure 3). During the same time period (i.e., between 2016 and 2018), we observed a steep
463 decline in *Sphagnum* N and P requirement (i.e., the N or P content of new tissue in g nutrient per
464 m^2 per year; Figure S3), in conjunction with *Sphagnum* mortality in the warmest treatments
465 (Norby and others 2019). The observed increase in shallow resin-available nutrients was related
466 (R^2 = 0.24 for NH_4-N and 0.09 for PO_4-P) to the decline in *Sphagnum* nutrient requirements in
467 the warmest treatments (Figure 5).

468 ***Monthly resin-available NH_4-N and PO_4-P increased exponentially in response to warming***

469 Given that nutrient response to warming was most notable in later treatment years, we
470 individually examined the Q_{10} dynamics in the last year of available data (2018, after 4 years of
471 whole-ecosystem warming, Figures 6 and S4, as well as across all treatment years, Table S5; see
472 Figures S5 and S6 for all data across all years). We found that a Q_{10} function explained the
473 warming response of NH_4-N and PO_4-P to increasing peat temperatures when observations from
474 across all warming and [CO_2] treatments were examined within a given microtopography and
475 peat depth, especially in deeper soil (Figures 6 and S4, respectively; observations from 2018

476 only). Significant Q_{10} values for increases in monthly resin-available nutrients with peat
477 temperature across all treatments ranged from ~3 to as much as ~9 in 2018, and higher when all
478 years were combined (Table S5); in turn, R_{12} values – the baseline amount of resin-available
479 nutrient at 12°C – tended to increase with peat depth (Table S5). While the ratio between
480 monthly resin-available N and P did not change significantly in response to warming, it did tend
481 to increase with peat depth (Figure 7).

482 ***Monthly resin-available nutrients and porewater nutrients were only somewhat correlated***

483 Cumulative monthly resin-available inorganic nutrients in hollows were somewhat correlated
484 with porewater inorganic nutrients in hollows across all enclosures and years 2015 – 2018 in
485 both shallower (Spearman's Rho = 0.30 and 0.32, for N and P, respectively, $P < 0.001$ for each)
486 and deeper peat (Spearman's Rho = 0.69 and 0.52 for N and P, respectively, $P < 0.0001$ for both
487 N and P; Figures 8, S7). Resin-available inorganic nutrients were somewhat correlated with
488 porewater organic nutrients (i.e., the difference between total N or P and inorganic N or P) in
489 shallower peat (Spearman's Rho = 0.34 and 0.30 for ON and OP respectively, $P < 0.0001$, for
490 both N and P) and in deeper peat (Spearman's Rho = 0.38 and 0.18, $P < 0.0001$ and $P = 0.004$,
491 for N and P, respectively; Figures 8, S7). Resin-available inorganic nutrients and total porewater
492 nutrients were also somewhat correlated, both in shallower peat (Spearman's Rho = 0.42 and
493 0.38 for TN and TP respectively, $P < 0.0001$, for both N and P) as well as in deeper peat
494 (Spearman's Rho = 0.66 and 0.52, $P < 0.0001$ for both N and P; Figures 8, S7).

495 **Discussion**

496 The controls over peatland C balance range from the environmental constraints of cold, acidic,
497 waterlogged peat to the interplay between C production and decomposition as mediated by
498 nutrient-limited plants and microbes (Bridgham and others 1998; Limpens and others 2008).

499 Many of these responses are underpinned by, or will affect, nutrient dynamics throughout the
500 peat profile. Here we found that after 4 years of whole-ecosystem warming and elevated [CO_2]
501 treatments: (1) Warming exponentially increased resin-available NH_4-N and PO_4-P, and the
502 magnitude of the response increased over time and varied across the microtopography of the bog
503 surface and with peat depth; (2) these dynamics were generally unaffected by elevated [CO_2];
504 and (3) relative increases in resin-available NH_4-N and PO_4-P with warming were similar,
505 though resin-available N/P ratios increased with peat depth.

506 ***Warming increased resin-available nutrients, but responses depended on microtopography***
507 ***and peat depth***

508 Warming exponentially increased resin-available NH_4-N and PO_4-P. The strength of this
509 response increased by an order of magnitude between the first and fourth years of whole-
510 ecosystem warming, and the increase in resin-available nutrients with warming was greatest in
511 deeper peat, at least early in the progression of experimental warming (Tables 1, Figures 2 and
512 3). However, we did not observe any significant effects of elevated [CO_2] on resin-available
513 NH_4-N or PO_4-P (Table 1; Figure 3). While evidence for peatland responses to elevated [CO_2] is
514 mixed, others have shown previously that elevated [CO_2] may not necessarily increase plant
515 production in nutrient-limited and *Sphagnum*-dominated bogs (Berendse and others 2001),
516 including the SPRUCE experimental enclosures (McPartland and others 2020, but see Norby and
517 others 2019). Thus, we may not expect an impact of elevated [CO_2] on nutrient cycling, or in
518 turn, nutrient responses may be weak or delayed. And while depth to water table almost certainly
519 plays a role in controlling resin-available nutrient dynamics throughout the peat profile,
520 especially given controls over rooting depth distribution and microbial activity, we saw little

warming-induced effects of water table level on resin-available nutrients (see *Supplementary Statistical Methods*).

Diminished competition at depth from shallowly-rooted vascular plant species, microbial communities, and *Sphagnum* mosses could explain the relatively stronger initial increases in resin-available nutrients with warming at deeper peat depths relative to shallower peat depths (Table 1; Figures 3, S5, S6). For example, prior to the initiation of warming, we found that the fine roots of the ericaceous shrubs and tree species in the S1 Bog were extremely shallowly distributed above the average summer water table level (Iversen and others 2018). And given that vertical transport of dissolved organic matter has been observed in the S1 Bog and in the SPRUCE experimental enclosures (Tfaily and others 2014; Tfaily and others 2018; Wilson and others 2021b), nutrients not acquired by plants in surface peat could accumulate at deeper peat depths (Griffiths & Sebestyen, 2016; Griffiths and others 2019). In turn, warming may lead to the destabilization and subsequent decomposition of organic matter at depth (e.g., Tfaily and others 2018; Wilson and others 2021a; AminiTabrizi and others 2022). Perhaps most importantly, prior to warming, the surface of the S1 Bog was carpeted by a layer of *Sphagnum* mosses (Norby and others 2019) which compete for and intercept nutrients at the peat surface from microbial mineralization, throughfall, and precipitation (Bähring and others 2017; Wang and others 2014).

Dynamics of resin-available nutrients in response to other nutrient pools

We saw a marked increase in NH_4-N and PO_4-P in the surface peat of the warmest treatments in recent years – especially in 2018 (Table 1, Figures 2, 3). This was unexpected given observed increases in above- and belowground production of ericaceous shrubs as well as in ectomycorrhizal fungal rhizomorphs in response to warming that would ostensibly increase

544 nutrient acquisition by bog vascular plant species (Defrenne and others 2021; Malhotra and
545 others 2020; McPartland and others 2020).

546 We hypothesize that the increase in nutrient availability in surface peat in the warmest plots in
547 later treatment years was linked to the mortality of *Sphagnum* mosses with warming at SPRUCE.
548 By 2018, the mosses were essentially decimated in the warmest enclosures from either peat
549 drying or shading from the strong growth response of ericaceous shrubs (Norby and others
550 2019). In particular, the largest increases in resin-available nutrients we observed were in the
551 warmest enclosures with the least *Sphagnum* nutrient demand (Figure 5). Furthermore, this large
552 increase in resin-available nutrients could also be related to the loss of *Sphagnum* capture of
553 atmospherically-derived nutrients (e.g., van der Heijden and others 2000; Wang and others
554 2017), which could explain the relatively greater relationship with resin-available N, which has
555 higher deposition rates than P (Salmon and others 2021). In turn, there may have been an
556 increase in nutrients released from dead and decaying *Sphagnum* necromass (Gerdol and others
557 2007). While not significant in the overall statistical model, there is some evidence that the
558 strong increase in surface nutrients with warming in more recent years was suppressed under
559 elevated [CO_2] (Table 1). We continue to monitor whether this pattern develops over time.

560 The relationship between nutrient availability and *Sphagnum* growth is bi-directional; while the
561 increase in inorganic nutrient availability in the surface peat of the warmest SPRUCE treatments
562 could be driven by the loss of *Sphagnum*, it could also be contributing to and potentially
563 accelerating *Sphagnum* loss. The detrimental impacts of increased nutrient availability on
564 *Sphagnum* growth and ground cover have been observed in a number of long-term nutrient
565 fertilization or nutrient deposition experiments in nutrient-poor peatlands (e.g., Limpens and
566 others 2011; Larmola and others 2013; Juutinen and others 2016; Levy and others 2018).

Shifting peatland vegetation composition with increased nutrient availability has implications for peatland ecosystem function, including increased peat subsidence and decreased capacity for peatland carbon storage (Franzén 2006; Limpens and others 2011; Larmola and others 2013; Kiheri and others 2020), and we are beginning to observe some of these impacts in the SPRUCE experimental treatments (Norby and others 2019; Hanson et al. 2020a).

Given that bogs are water-saturated ecosystems where much of the belowground peat environment tends to be perennially inundated with porewater, we compared resin-available nutrient dynamics to porewater nutrient dynamics. We found that resin-available NH_4-N and PO_4-P were only somewhat correlated with porewater inorganic N and P (Figures 8 and S7, respectively), likely indicating that these metrics of nutrient dynamics represent different spatial and temporal components of the bog nutrient cycles. In contrast to the 'root-like' acquisition of ion-exchange resins, porewater, similar to one-time soil extractions, represents a snapshot, or pool, of residual nutrients that are not currently immobilized in plant or microbial biomass (Bourbonniere, 2009; Bridgham and others 2001; Griffiths and others 2019). Furthermore, previous work has shown that ion-exchange resins may be good integrators of nutrient 'hot moments' that occur over time (Darrouzet-Nardi and Bowman 2011), while these dynamic fluxes could either be missed with periodic sampling or assigned outsized importance. On the other hand, lateral outflow could be a good integrator of nutrient 'hot spots' across the plot (e.g., Sebestyen and Griffiths 2016; Curtinrich and others 2021). We did observe stronger correlations between resin-available and porewater nutrients in deeper peat (Figures 8, S7), potentially due to the accumulation of nutrients transported downward through the peat profile (e.g., Griffiths & Sebestyen, 2016) or the destabilization of organic matter at depth with warmer temperatures (e.g., Tfaily and others 2018; Wilson and others 2021a; AminiTabrizi and others 2022).

590 Organic nutrients have been hypothesized to be a potential nutrient source in cold, nutrient-
591 limited ecosystems (Kielland, 1994; Kielland and others 2006; Raab and others 1999; Schimel
592 and others 2004), including in the S1 Bog (Salmon and others 2021). However, ion-exchange
593 resins do not allow us to make any conclusions with regard to plant-available organic nutrients,
594 as inorganic resin-available nutrients were not well-correlated with porewater organic N and P
595 (Figure 8). While porewater organic N and P were a large fraction of the total dissolved nutrient
596 pools (~81% ± 19 SD for N and 46% ± 29 SD for P across all collection dates and depths), much
597 of this porewater organic nutrient pool likely represents polymers too large for plants to directly
598 uptake (Schimel & Bennett, 2004). Furthermore, increasing mineral N can lead to decreasing
599 preference for organic N acquisition (Cott and others 2020), though mycorrhizal partnerships can
600 change this dynamic (Defrenne and others 2021).

601 In addition to N and P, other macronutrients limit plant growth in peatlands (e.g., Hoosbeek and
602 others 2002; Larmola and others 2013; Wang and others 2017; Levy and others 2018), and the
603 dynamics of multiple nutrient cations in porewater are being quantified over space and time at
604 the S1 Bog as well as in the SPRUCE experimental enclosures (e.g., Griffiths and Sebestyen
605 2016; Griffiths and others 2019). Preliminary evidence indicates that the outflow of nutrients
606 such as Ca and Fe have increased with warming in the SPRUCE experimental treatments
607 (Curtinrich and others 2021).

608 ***Warming increased the availability of NH_4-N and PO_4-P at similar rates***

609 We did not find any significant differences in the relative responses of resin-available NH_4-N
610 and PO_4-P to warming (Table 1; Figures 2, 3, and 7). The ratio of cumulative annual available
611 NH_4-N to PO_4-P was highly variable, but averaged 12.6 (± 17.2 SD) across all depths and years,
612 close to the average N/P ratio of plant biomass at the S1 Bog (~12; Salmon and others 2021).

613 The cumulative annual resin-available N/P ratio tended to be slightly lower than the average N/P
614 ratio of peat measured in the S1 Bog (0 to 30 cm peat depth, averaged across hummocks and
615 hollows, 18 ± 4 SD; Salmon and others 2021) and in a recent review spanning a range of boreal
616 bogs (0 – 50 cm peat depth, 24.5 ± 0.8; Wang and others 2015). This could indicate that there
617 was a relatively more limited NH_4-N supply compared to PO_4-P in the pool of nutrients that were
618 mineralized from peat and became resin-available between 2014 and 2018 (potentially due to
619 low activation energy of N-acquiring enzymes compared to P observed in the S1 Bog; Steinweg
620 and others 2018). In turn, it could be that NH_4-N tended to be more limiting for plant and
621 microbial growth in the SPRUCE enclosures (Cleveland and others 2007; Salmon and others
622 2021), and thus there was more competition from plants and microbes with the ion-exchange
623 resins for NH_4-N compared to PO_4-P. While the cumulative annual resin-available N/P ratio did
624 not change significantly in response to warming, resin-available N/P ratio did tend to increase
625 with peat depth (Tables 1 and S3; Figure 7), indicating an increase in P limitation in deeper peat.
626 This increasing N/P ratio with depth has been observed in the peat profile in the SPRUCE bog
627 (Salmon and others 2021) as well as in other bogs (Wang and others 2015). One theory regarding
628 these depth dynamics is that P is strongly limiting to microbial growth in peatlands and is tightly
629 cycled at the peat surface, whereas N is buried and accumulates with peat depth (Bridgham and
630 others 1998; Hill and others 2014; Steinweg and others 2018; Tfaily and others 2014; Wang and
631 others 2015).

632 ***Nutrient availability increased exponentially with peat temperature***

633 In addition to examining the response of NH_4-N and PO_4-P to warming and elevated [CO_2] at an
634 annual level, we were also able to look at the more highly-resolved resin-available nutrient
635 dynamics at an ~monthly (28-day) timestep. We fit Q_{10} temperature response functions to

consider the temperature cues of monthly nutrient availability (similar to soil CO_2 efflux, as in Hanson and others 2000) and to provide an important model parameter that may be used to simulate or benchmark nutrient availability in land surface models (e.g., Shi and others 2021). A Q_{10} function explained a large fraction of variation in resin-available NH_4-N and PO_4-P with increasing peat temperature in deeper peat, where the Q_{10} parameter was quite large (ranging from 2.5 to 51.4 across all years, microtopographic positions, and peat depths; Figures 6 and S4, Table S5). However, the Q_{10} function was a poor fit in surface soils, potentially due to the influence of competition from plants and microbes on nutrient accumulation on ion-exchange resins or potential loss of nutrients to deeper peat.

Implications for understanding and modeling peatland responses to warming

A hypothesized indirect response of ecosystems to warming is an increase in microbial nutrient mineralization, and therefore plant-available nutrients, that leads to increased plant growth and changing plant community composition, with follow-on impacts on ecosystem C storage (Bragazza and others 2013; Liu and others 2020; Rustad and others 2001; Salazar and others 2020). We use terrestrial biosphere models such as ELM-SPRUCE to conceptualize and test these hypotheses – along with other mechanisms such as plant physiology and nutrient requirements – but models must be compared with and validated against experimental observations. Annual cumulative net nutrient mineralization predicted by ELM-SPRUCE reflects nutrient availability on an annual time scale and is a foundation for modeled plant and soil responses to warming. We compared model-predicted net nutrient mineralization with our long-term and highly-resolved observations of resin-available nutrient dynamics; these fluxes have been qualitatively compared previously across a number of peatland ecosystems to inform understanding of peatland nutrient dynamics (as in Bridgham and others 2001).

Similar to the patterns observed in resin-available nutrients, ELM-SPRUCE projected a sustained and exponential increase in net N and P mineralization in response to warming, with no discernable effects of elevated [CO_2] (Figure 4). However, the magnitudes of the modeled increases in net N and P mineralization with increasing peat temperature were much lower than the responses observed in resin-available nutrients (e.g., the calculated Q_{10} responses for model output of net nutrient mineralization ranged between ~1.5 and 5 across peat depths and microtopographic positions, compared to the much higher observed Q_{10} responses in resin-available nutrients; Figures 6 and S4, Table S5). This could be because the Q_{10} warming response of microbial decomposition is underestimated by the model, or in turn because models do not incorporate potential 'hot moments' that are integrated by ion-exchange resins over time (e.g., Darrouzet-Nardi and Bowman 2011).

Model predictions of increases in annual cumulative net N and P mineralization with warming were greater in depressed hollows, likely due to model-predicted drying in the hollows with warming (a response not observed at SPRUCE between 2014 and 2018), which increases organic matter decomposition. ELM-SPRUCE also predicted greater net nutrient mineralization in hollows on average, similar to the observed patterns in resin-available nutrients, though the mechanism for this was less clear and may be related to relatively less root activity in the hollows than hummocks (e.g., Iversen and others 2018).

ELM-SPRUCE predicted a decrease in net N and P mineralization with depth (Figure 4), in contrast to observations of increasing resin-available nutrients with depth, across all treatments (Table 1, Figure 3). ELM-SPRUCE encodes a decline in microbial activity with peat depth, but we hypothesize that the model is either not capturing the potential transport of dissolved organic matter (and associated nutrients) downward through the peat profile (e.g., Griffiths & Sebestyen,

2016) or not capturing the destabilization and subsequent decomposition of organic matter at depth with warmer temperatures (e.g., Tfaily and others 2018; Wilson and others 2021a; AminiTabrizi and others 2022). The absence of either mechanism could explain why the model does not predict an accumulation of nutrients in deeper peat. Continued iteration between experimental observations and model predictions, which are based on underlying model parameterization and process conceptualization, can help to improve our projections of peatland responses to climate change across the world.

Conclusions

The SPRUCE experimental warming by elevated [CO_2] manipulation is the largest of its kind, allowing us to examine the whole-ecosystem impacts of a gradient of warming and potential interaction with rising atmospheric [CO_2] in a peatland ecosystem. We found that warming exponentially increased plant-available nutrients, but that the magnitude of the response varied over time and across the microtopography of the bog surface and with peat depth. To-date these patterns remained generally unaffected by elevated [CO_2]. Furthermore, complex interactions are suggested by the simultaneous long-term loss of the *Sphagnum* community and the relatively sudden increase in the availability of nutrients in surface peat, likely driven by both biotic and abiotic factors. Predictions of peatland nutrient availability in land surface models under climate change scenarios must account for dynamic changes in nutrient acquisition by plants and microbes, as well as microtopography and peat depth.

Acknowledgements

The SPRUCE experiment is supported by the Biological and Environmental Research program in the United States Department of Energy's Office of Science. Oak Ridge National Laboratory

is managed by UT-Battelle, LLC, for the United States Department of Energy under contract DE-AC05-00OR22725. We thank Sarah Bellaire, Alana Burnham, Kelsey Carter, Ingrid Slette, and Nathan Stenson for their help in the field or laboratory. We also thank the editorial staff and anonymous reviewers for their helpful feedback. The contributions of SDS and funding for the Marcell Experimental Forest and laboratory analysis by the Forest Service were provided by the Northern Research Station of the United States Department of Agriculture Forest Service.

Conflicts of Interest

The authors declare no competing interest.

References

Aerts R, Cornelissen JHC, Dorrepaal E. 2006. Plant performance in a warmer world: General responses of plants from cold, northern biomes and the importance of winter and spring events. Plant Ecology 182: 65-77.

AminiTabrizi R, Dontsovaa K, Graf Gracheta N, Tfaily MM. 2022. Elevated temperatures drive abiotic and biotic degradation of organic matter in a peat bog under oxic conditions. Science of The Total Environment 804: 150045.

APHA. 2017. Standard methods for the examination of water and wastewater, 23rd ed. Washington, DC.

Bähring A, Fichtner A, Friedrich U, von Oheimb G, Härdtle W. 2017. Bryophytes and organic layers control uptake of airborne nitrogen in low-N environments. Frontiers in Plant Science 8: 2080.

Barbier C, Hanson PJ, Todd DE, Belcher D, Jekabson EW, Thomas WK, Riggs J. 2013. Air flow and heat transfer in a temperature-controlled open top enclosure. American Society of Mechanical Engineers 7: 9780791845233.

Berendse F, Van Breemen N, Rydin H, Buttler A, Heijmans M, Hoosbeek MR, Lee JA, Mitchell E, Saarinen T, Vasander H, Wallén B. 2001. Raised atmospheric CO_2 levels and increased N deposition cause shifts in plant species composition and production in *Sphagnum* bogs. Global Change Biology 7: 591-598.

Bourbonniere RA. 2009. Review of water chemistry research in natural and disturbed peatlands. Canadian Water Resources Journal 34: 393-414.

Bragazza L, Freeman C, Jones T, Rydin H, Limpens J, Fenner N, Ellis T, Gerdol R, Hájek M, Hájek T, Iacumin P, Kutnar L, Tahvanainen T, Toberman H. 2006. Atmospheric nitrogen deposition promotes carbon loss from peat bogs. Proceedings of the National Academy of Sciences of the United States of America 103: 19386-19389.

Bragazza L, Parisod J, Buttler A, Bardgett RD. 2013. Biogeochemical plant–soil microbe feedback in response to climate warming in peatlands. Nature Climate Change 3: 273-277.

Bridgham SD, Megonigal JP, Keller JK, Bliss NB, Trettin C. 2006. The carbon balance of North American wetlands. Wetlands 26: 889-916.

Bridgham SD, Pastor J, Dewey B, Weltzin JF, Updegraff K. 2008. Rapid carbon response of peatlands to climate change. Ecology 89: 3041-3048.

Bridgham SD, Updegraff K, Pastor J. 1998. Carbon, nitrogen, and phosphorus mineralization in northern wetlands. Ecology 79: 1545-1561.

Bridgham SD, Updegraff K, Pastor J. 2001. A comparison of nutrient availability indices along an ombrotrophic-minerotrophic gradient in Minnesota wetlands. Soil Science Society of America Journal 65: 259-269.

Burrows SM, Maltrud M, Yang X, Zhu Q, Jeffery N, Shi X, Ricciuto D, Wang S, Bisht G, Tang J, Wolfe J, Harrop BE, Singh B, Brent S, Baldwin S, Zhou T, Cameron-Smith P, Keen N, Collier N, Xu M, Hunke EC, Elliott SM, Turner AK, Li H, Wang H, Golaz J-C, Bond-Lamberty B, Hoffman FM, Riley WJ, Thornton PE, Calvin K, Leung LR. 2020. The DOE E3SM v1.1 Biogeochemistry configuration: Description and simulated ecosystem-climate responses to historical changes in forcing. Journal of Advances in Modeling Earth Systems 12: e2019MS001766.

Cleveland CC, Liptzin D. 2007. C:N:P stoichiometry in soil: is there a "Redfield ratio" for the microbial biomass? Biogeochemistry 85: 235-252.

Cott GM, Jansen MAK, Megonigal JP. 2020. Uptake of organic nitrogen by coastal wetland plants under elevated CO_2. Plant and Soil 450: 521-535.

Curtinrich HJ, Sebestyen SD, Griffiths NA, Hall SJ. 2021. Warming stimulates iron-mediated carbon and nutrient cycling in mineral-poor peatlands. Ecosystems.

Darrouzet-Nardi A, Bowman WD. 2011. Hot spots of inorganic nitrogen availability in an alpine-subalpine ecosystem, Colorado Front Range. Ecosystems 14: 848-863.

de Graaff MA, van Groenigen KJ, Six J, Hungate B, van Kessel C. 2006. Interactions between plant growth and soil nutrient cycling under elevated CO_2: a meta-analysis. Global Change Biology 12: 2077-2091.

Defrenne CE, Childs J, Fernandez CW, Taggart M, Nettles WR, Allen MF, Hanson PJ, Iversen CM. 2021. High-resolution minirhizotrons advance our understanding of root-fungal dynamics in an experimentally warmed peatland. Plants, People, Planet 3: 640-652.

Eppinga MB, Rietkerk M, Belyea LR, Nilsson MB, De Ruiter PC, Wassen MJ. 2010. Resource contrast in patterned peatlands increases along a climatic gradient. Ecology 91: 2344-2355.

Fenner N, Ostle NJ, McNamara N, Sparks T, Harmens H, Reynolds B, Freeman C. 2007. Elevated CO_2 effects on peatland plant community carbon dynamics and DOC production. Ecosystems 10: 635-647.

Finzi AC, Norby RJ, Calfapietra C, Gallet-Budynek A, Gielen B, Holmes WE, Hoosbeek MR, Iversen CM, Jackson RB, Kubiske ME, Ledford J, Liberloo M, Oren R, Polle A, Pritchard S, Zak DR, Schlesinger WH, Ceulemans R. 2007. Increases in nitrogen uptake rather than nitrogen-use efficiency support higher rates of temperate forest productivity under elevated CO_2. Proceedings of the National Academy of Sciences 104: 14014-14019.

Franzén LG. 2006. Increased decomposition of subsurface peat in Swedish raised bogs: Are temperate peatlands still net sinks of carbon? Mires and Peat 1: 03.

Gerdol R, Petraglia A, Bragazza L, Iacumin P, Brancaleoni L. 2007. Nitrogen deposition interacts with climate in affecting production and decomposition rates in *Sphagnum* mosses. Global Change Biology 13: 1810-1821.

Giblin AE, Laundre JA, Nadelhoffer KJ, Shaver GR. 1994. Measuring nutrient availability in arctic soils using ion exchange resins: A field test. Soil Science Society of America Journal 58: 1154-1162.

Gorham E. 1991. Northern peatlands: Role in the carbon cycle and probably responses to climatic warming. Ecological Applications 1: 182-195.

Graham JD, Glenn NF, Spaete LP, Hanson PJ. 2020. Characterizing peatland microtopography using gradient and microform-based approaches. Ecosystems 23: 1464-1480.

Griffiths NA, Sebestyen SD. 2016. Dynamic vertical profiles of peat porewater chemistry in a northern peatland. Wetlands 36: 1119-1130.

Griffiths NA, Hanson PJ, Ricciuto DM, Iversen CM, Jensen AM, Malhotra A, McFarlane KJ, Norby RJ, Sargsyan K, Sebestyen SD, Shi X, Walker AP, Ward EJ, Warren JM, Weston DJ. 2017. Temporal and spatial variation in peatland carbon cycling and implications for interpreting responses of an ecosystem-scale warming experiment. Soil Science Society of America Journal 81: 1668-1688.

Griffiths NA, Hook LA, Hanson PJ. 2016a. SPRUCE S1 Bog and SPRUCE experiment location survey results, 2015 and 2020. Oak Ridge National Laboratory, TES SFA, U.S. Department of Energy, Oak Ridge, Tennessee, U.S.A. https://doi.org/10.3334/CDIAC/spruce.015

Griffiths NA, Sebestyen SD, Oleheiser KC. 2019. Variation in peatland porewater chemistry over time and space along a bog to fen gradient. Science of the Total Environment 697: 14.

Griffiths NA, Sebestyen SD, Oleheiser KC, Stelling JM, Pierce CE, Nater EA, Toner BM, Kolka RK. 2016b. SPRUCE Porewater Chemistry Data for Experimental Plots Beginning in 2013, 3rd edition. Oak Ridge National Laboratory, TES SFA, U.S. Department of Energy, Oak Ridge, Tennessee, U.S.A. https://doi.org/10.3334/CDIAC/spruce.028

Gu Q, Grogan P. 2020. Nutrient availability measurement techniques in arctic tundra soils: in situ ion exchange membranes compared to direct extraction. Plant and Soil 454: 359-378.

Hanson PJ, Edwards NT, Garten CT, Andrews JA. 2000. Separating root and soil microbial contributions to soil respiration: A review of methods and observations. Biogeochemistry 48: 115-146.

Hanson PJ, Griffiths NA, Iversen CM, Norby RJ, Sebestyen SD, Phillips JR, Chanton JP, Kolka RK, Malhotra A, Oleheiser KC, Warren JM, Shi X, Yang X, Mao J, Ricciuto DM. 2020a. Rapid net carbon loss from a whole-ecosystem warmed peatland. AGU Advances 1: e2020AV000163.

Hanson PJ, Phillips JR, Nettles WR, Pearson KJ, Hook LA. 2020b. SPRUCE plot-level water table data assessments for absolute elevations and height with respect to mean hollows beginning in 2015. Oak Ridge National Laboratory, TES SFA, U.S. Department of Energy, Oak Ridge, Tennessee, U.S.A. https://doi.org/10.25581/spruce.079/1608615

Hanson PJ, Riggs JS, Nettles WR, Krassovski MB, Hook LA. 2016. SPRUCE whole ecosystems warming (WEW) environmental data beginning August 2015. Oak Ridge National Laboratory, TES SFA, U.S. Department of Energy, Oak Ridge, Tennessee, U.S.A. https://doi.org/10.3334/CDIAC/spruce.032

Hanson PJ, Riggs JS, Nettles WR, Phillips JR, Krassovski MB, Hook LA, Gu L, Richardson AD, Aubrecht DM, Ricciuto DM, Warren JM, Barbier C. 2017. Attaining whole-ecosystem warming using air and deep-soil heating methods with an elevated CO_2 atmosphere. Biogeosciences 14: 861-883.

Harrison XA, Donaldson L, Correa-Cano ME, Evans J, Fisher DN, Goodwin CED, Robinson BS, Hodgson DJ, Inger R. 2018. A brief introduction to mixed effects modelling and multi-model inference in ecology. PeerJ 6: e4794.

Hedwall P-O, Brunet J, Rydin H. 2017. Peatland plant communities under global change: negative feedback loops counteract shifts in species composition. Ecology 98: 150-161.

Herndon EM, Kinsman-Costello L, Duroe KA, Mills J, Kane ES, Sebestyen SD, Thompson AA, Wullschleger SD. 2019. Iron (Oxyhydr)Oxides serve as phosphate traps in tundra and boreal peat soils. Journal of Geophysical Research: Biogeosciences 124: 227-246.

Hill BH, Elonen CM, Jicha TM, Kolka RK, Lehto LLP, Sebestyen SD, Seifert-Monson LR. 2014. Ecoenzymatic stoichiometry and microbial processing of organic matter in northern bogs and fens reveals a common P-limitation between peatland types. Biogeochemistry 120: 203-224.

Hoosbeek MR, Van Breemen N, Vasander H, Buttler A, Berendse F. 2002. Potassium limits potential growth of bog vegetation under elevated atmospheric CO_2 and N deposition. Global Change Biology 8: 1130-1138.

IPCC (2021). Climate Change 2021: The Physical Science Basis. Contribution of Working Group I to the Sixth Assessment Report of the Intergovernmental Panel on Climate Change [Masson-Delmotte V, P Zhai, A Pirani, SL Connors, C Péan, S Berger, N Caud, Y Chen, L Goldfarb, MI Gomis, M Huang, K Leitzell, E Lonnoy, JBR Matthews, TK Maycock, T Waterfield, O Yelekçi, R Yu, B Zhou (eds.)]. Cambridge University Press. In Press.

Iversen CM, Bridgham SD, Kellogg LE. 2010. Scaling plant nitrogen use and uptake efficiencies in response to nutrient addition in peatlands. Ecology 91: 693-707.

Iversen CM, Childs J, Norby RJ, Ontl TA, Kolka RK, Brice DJ, McFarlane K, Hanson PJ. 2018. Fine-root growth in a forested bog is seasonally dynamic, but shallowly distributed in nutrient-poor peat. Plant and Soil 424: 123-143.

Iversen CM, Hanson PJ, Brice DJ, Phillips JR, McFarlane KJ, Hobbie EA, Kolka RK. 2014. SPRUCE peat physical and chemical characteristics from experimental plot cores, 2012. Oak Ridge National Laboratory, TES SFA, U.S. Department of Energy, Oak Ridge, Tennessee, U.S.A. https://doi.org/10.3334/CDIAC/spruce.005

Iversen CM, Latimer J, Burnham A, Brice DJ, Childs J, Vander Stel HM. 2017. SPRUCE Plant-Available Nutrients Assessed with Ion-Exchange Resins in Experimental Plots, Beginning in 2013. Carbon Dioxide Information Analysis Center, Oak Ridge National Laboratory, U.S. Department of Energy, Oak Ridge, Tennessee, U.S.A. http://dx.doi.org/10.3334/CDIAC/spruce.036.

Juutinen S, Moore TR, Laine AM, Bubier JL, Tuittila E-S, De Young A, Chong M. 2016. Responses of the mosses *Sphagnum capillifolium* and *Polytrichum strictum* to nitrogen deposition in a bog: Growth, ground cover, and CO_2 exchange. Botany 94: 127-138.

Keller JK, Bauers AK, Bridgham SD, Kellogg LE, Iversen CM. 2006. Nutrient control of microbial carbon cycling along an ombrotrophic-minerotrophic peatland gradient. Journal of Geophysical Research: Biogeosciences, 111: G3.

Keuper F, van Bodegom PM, Dorrepaal E, Weedon JT, van Hal J, van Logtestijn RSP, Aerts R. 2012. A frozen feast: thawing permafrost increases plant-available nitrogen in subarctic peatlands. Global Change Biology 18: 1998-2007.

Kielland K. 1994. Amino-acid absorption by arctic plants – Implications for plant nutriention and nitrogen cycling. Ecology 75: 2373-2383.

Kielland K, McFarland J, Olson K. 2006. Amino acid uptake in deciduous and coniferous taiga ecosystems. Plant and Soil 288: 297-307.

Kiheri H, Velmala S, Pennanen T, Timonen S, Sietiö O-M, Fritze H, Heinonsalo J, van Dijk N, Dise N, Larmola T. 2020. Fungal colonization patterns and enzymatic activities of peatland ericaceous plants following long-term nutrient addition. Soil Biology and Biochemistry 147: 107833.

Koerselman W, Arthur FMM. 1996. The Vegetation N:P Ratio: a new tool to detect the nature of nutrient limitation. Journal of Applied Ecology 33: 1441-1450.

Larmola T, Bubier JL, Kobyljanec C, Basiliko N, Juutinen S, Humphreys E, Preston M, Moore TR. 2013. Vegetation feedbacks of nutrient addition lead to a weaker carbon sink in an ombrotrophic bog. Global Change Biology 19: 3729-3739.

Levy P, van Dijk N, Gray A, Sutton M, Jones M, Leeson S, Dise N, Leith I, Sheppard L. 2019. Response of a peat bog vegetation community to long-term experimental addition of nitrogen. Journal of Ecology 107: 1167-1186.

Limpens J, Berendse F, Blodau C, Canadell JG, Freeman C, Holden J, Roulet N, Rydin H, Schaepman-Strub G. 2008. Peatlands and the carbon cycle: from local processes to global implications – a synthesis. Biogeosciences 5: 1475-1491.

Limpens J, Granath G, Gunnarsson U, Aerts R, Bayley S, Bragazza L, Bubier J, Buttler A, van den Ber LJL, Francez A-J, Gerdol R, Grosvernier P, Heijmans MMPD, Hoosbeek MR, Hotes S, Ilomets M, Leith I, Mitchell EAD, Moore T, Nilsson MB, Nordbakken J-F, Rochefort L, Rydin H, Sheppard LJ, Thormann M, Wiedermann MM, Williams BL, Xu B. 2011. Climatic modifiers of the response to N deposition in peat-forming *Sphagnum* mosses: a meta-analysis. New Phytologist 191: 496-507.

Liu H, Xu X, Zhou C, Zhao J, Li B, Nie M. 2020. Geographic linkages of root traits to salt marsh productivity. Ecosystems.

Lloyd J, Taylor JA. 1994. On the temperature dependence of soil respiration. Functional Ecology 8: 315-323.

Mack MC, Schuur EAG, Bret-Harte MS, Shaver GR, Chapin FS. 2004. Ecosystem carbon storage in arctic tundra reduced by long-term nutrient fertilization. Nature 431: 440-443.

Malhotra A, Brice DJ, Childs J, Graham JD, Hobbie EA, Vander Stel H, Feron SC, Hanson PJ, Iversen CM. 2020. Peatland warming strongly increases fine-root growth. Proceedings of the National Academy of Sciences 117: 17627-17634.

Malhotra A, Moore TR, Limpens J, Roulet NT. 2018. Post-thaw variability in litter decomposition best explained by microtopography at an ice-rich permafrost peatland. Arctic, Antarctic, and Alpine Research 50: e1415622.

McFarlane KJ, Hanson PJ, Iversen CM, Phillips JR, Brice DJ. 2018. Local spatial heterogeneity of Holocene carbon accumulation throughout the peat profile of an ombrotrophic northern Minnesota bog. Radiocarbon 60: 941-962.

McPartland MY, Montgomery RA, Hanson PJ, Phillips JR, Kolka R, Palik B. 2020. Vascular plant species response to warming and elevated carbon dioxide in a boreal peatland. Environmental Research Letters 15: 12.

Medlyn BE, Zaehle S, De Kauwe MG, Walker AP, Dietze MC, Hanson PJ, Hickler R, Jain AK, Luo Y, Parton W, Prentice IC, Thornton PE, Wang S, Wang Y-P, Weng E, Iversen CM, McCarthy HR, Warren JM, Oren R, Norby RJ. 2015. Using ecosystem experiments to improve vegetation models. Nature Climate Change 5: 528-534.

Milla R, Cornelissen JHC, van Logtestijn RSP, Toet S, Aerts R. 2006. Vascular plant responses to elevated CO_2 in a temperate lowland *Sphagnum* peatland. Plant Ecology 182: 13-24.

Mooshammer M, Hofhansl F, Frank AH, Wanek,W, Hämmerle I, Leitner S, Schnecker J, Wild B, Watzka M, Keiblinger KM, Zechmeister-Boltenstern S, Richter A. 2017. Decoupling of microbial carbon, nitrogen, and phosphorus cycling in response to extreme temperature events. Science Advances 3: e1602781.

Munir TM, Khadka B, Xu B, Strack M. 2017. Mineral nitrogen and phosphorus pools affected by water table lowering and warming in a boreal forested peatland. Ecohydrology 10: 15.

Murphy MT, Moore TR. 2010. Linking root production to aboveground plant characteristics and water table in a temperate bog. Plant and Soil 336: 219-231.

Nichols JE, Peteet DM. 2019. Rapid expansion of northern peatlands and doubled estimate of carbon storage. Nature Geoscience 12: 917-921.

Norby RJ, Childs J. 2018. SPRUCE: Sphagnum productivity and community composition in the SPRUCE experimental Plots. Oak Ridge National Laboratory, TES SFA, U.S. Department of Energy, Oak Ridge, Tennessee, U.S.A. https://doi.org/10.25581/spruce.049/1426474

Norby RJ, Childs J, Brice DJ. 2020. SPRUCE: Sphagnum carbon, nitrogen and phosphorus concentrations in the SPRUCE experimental plots. Oak Ridge National Laboratory, TES SFA, U.S. Department of Energy, Oak Ridge, Tennessee, U.S.A. https://doi.org/10.25581/spruce.084/1647361

Norby RJ, Childs J, Hanson PJ, Warren JM. 2019. Rapid loss of an ecosystem engineer: *Sphagnum* decline in an experimentally warmed bog. Ecology and Evolution 9: 12571-12585.

Olid C, Nilsson MB, Eriksson T, Klaminder J. 2014. The effects of temperature and nitrogen and sulfur additions on carbon accumulation in a nutrient-poor boreal mire: Decadal effects assessed using 210Pb peat chronologies. Journal of Geophysical Research: Biogeosciences 119: 392-403.

Parsekian AD, Slater L, Ntarlagiannis D, Nolan J, Sebesteyen SD, Kolka RK, Hanson PJ. 2012. Uncertainty in peat volume and soil carbon estimated using ground-penetrating radar and probing. Soil Science Society of America Journal 76: 1911-1918.

R Core Team. 2021. R: A language and environment for statistical computing. R Foundation for Statistical Computing, Vienna, Austria. https://www.R-project.org/.

Raab TK, Lipson DA, Monson RK. 1999. Soil amino acid utilization among species of the Cyperaceae: Plant and soil processes. Ecology 80: 2408-2419.

Richardson AE, Barea JM, McNeill AM, Prigent-Combaret C. 2009. Acquisition of phosphorus and nitrogen in the rhizosphere and plant growth promotion by microorganisms. Plant and Soil 321: 305-339.

Richardson CJ. 1985. Mechanisms controlling phosphorus retention capacity in freshwater wetlands. Science 228: 1424-1427.

Rustad LE, Campbell JL, Marion GM, Norby RJ, Mitchell MJ, Hartley AE, Cornelissen J, Gurevitch J, GCTE-NEWS. 2001. A meta-analysis of the response of soil respiration, net nitrogen mineralization, and aboveground plant growth to experimental ecosystem warming. Oecologia 126: 543-562.

Salazar A, Rousk K, Jónsdóttir IS, Bellenger J-P, Andrésson ÓS. 2020. Faster nitrogen cycling and more fungal and root biomass in cold ecosystems under experimental warming: a meta-analysis. Ecology 101: e02938.

Salmon VG, Brice DJ, Brigham S, Childs J, Graham JD, Griffiths NA, Hofmockel K, Iversen CM, Jicha TM, Kolka RK, Kostka JE, Malhotra A, Norby RJ, Phillips JR, Ricciuto D, Schadt CW, Sebestyen SD, Shi X, Walker AP, Warren JM, Weston DJ, Yang X, Hanson PJ. 2021. Nitrogen and phosphorus cycling in an ombrotrophic peatland: A benchmark for assessing change. Plant and Soil 466: 649–674.

Schimel JP, Bennett J. 2004. Nitrogen mineralization: Challenges of a changing paradigm. Ecology 85: 591-602.

Seay S. 2018. Peatlands hold carbon even in warming environment. Oak Ridge National Laboratory Review 51: 20-23.

Sebestyen SD, Dorrance C, Olson DM, Verry ES, Kolka RK, Elling AE, Kyllander R. 2011. Long-term monitoring sites and trends at the Marcell Experimental Forest. In R. K.Kolka, S. D. Sebestyen, a. E. S. Verry, & K. N. Brooks (Eds.), Peatland Biogeochemistry and Watershed Hydrology at the Marcell Experimental Forest (pp. 15-72). New York, NY: CRC Press, Inc.

Sebestyen SD, Griffiths NA. 2016. SPRUCE enclosure corral and sump system: Description, operation, and calibration. Climate Change Science Institute, Oak Ridge National Laboratory, U.S. Department of Energy, Oak Ridge, Tennessee, U.S.A. http://dx.doi.org/10.3334/CDIAC/spruce.030

Shi X, Ricciuto DM, Thornton PE, Xu X, Yuan F, Norby RJ, Walker AP, Warren JM, Mao J, Hanson PJ, Meng L, Weston D, Griffiths NA. 2021. Extending a land-surface model with Sphagnum moss to simulate responses of a northern temperate bog to whole ecosystem warming and elevated CO_2. Biogeosciences 18: 467-486.

Shi X, Thornton PE, Ricciuto DM, Hanson PJ, Mao J, Sebestyen SD, Griffiths NA, Bisht G. 2015. Representing northern peatland microtopography and hydrology within the Community Land Model. Biogeosciences 12: 6463-6477.

Skogley EO, Dobermann A. 1996. Synthetic ion-exchange resins: Soil and environmental studies. Journal of Environmental Quality 25: 13-24.

Spohn M, Kuzyakov Y. 2013. Phosphorus mineralization can be driven by microbial need for carbon. Soil Biology and Biochemistry 61: 69-75.

Steinweg JM, Kostka JE, Hanson PJ, Schadt CW. 2018. Temperature sensitivity of extracellular enzymes differs with peat depth but not with season in an ombrotrophic bog. Soil Biology and Biochemistry 125: 244-250.

Tfaily MM, Cooper WT, Kostka JE, Chanton PR, Schadt CW, Hanson PJ, Iversen CM, Chanton JP. 2014. Organic matter transformation in the peat column at Marcell Experimental Forest: Humification and vertical stratification. Journal of Geophysical Research-Biogeosciences 119: 661-675.

Tfaily MM, Wilson RM, Cooper WT, Kostka JE, Hanson P, Chanton JP. 2018. Vertical stratification of peat pore water dissolved organic matter composition in a peat bog in northern Minnesota. Journal of Geophysical Research: Biogeosciences 123: 479-494.

Toet S, Cornelissen JHC, Aerts R, van Logtestijn RSP, de Beus M, Stoevelaar R. 2006. Moss responses to elevated CO_2 and variation in hydrology in a temperate lowland peatland. Plant Ecology 182: 27-40.

van der Heijden E, Verbeek SK, Kuiper PJC. 2000. Elevated atmospheric CO_2 and increased nitrogen deposition: effects on C and N metabolism and growth of the peat moss *Sphagnum recurvum* P. Beauv. var. *mucronatum* (Russ.) Warnst. Global Change Biology 6: 201-212.

Vitousek PM, Howarth RW. 1991. Nitrogen limitation on land and in the sea: How can it occur? Biogeochemistry 13: 87-115.

Vitt DH, Chee,W-L. 1990. The relationships of vegetation to surface water chemistry and peat chemistry in fens of Alberta, Canada. Vegetatio 89: 87-106.

Walker AP, De Kauwe MG, Bastos A, Belmecheri S, Georgiou K, Keeling RF . . . Zuidema PA. 2021. Integrating the evidence for a terrestrial carbon sink caused by increasing atmospheric CO_2. New Phytologist 229: 2413-2445.

Walker TW, Syers JK. 1976. The fate of phosphorus during pedogenesis. Geoderma 15: 1-19.

Wang J, Shi F, Xu B, Wang Q, Wu Y, Wu N. 2014. Uptake and recovery of soil nitrogen by bryophytes and vascular plants in an alpine meadow. Journal of Mountain Science 11: 475-484.

Wang M, Moore TR. 2014. Carbon, nitrogen, phosphorus, and potassium stoichiometry in an ombrotrophic peatland reflects plant functional type. Ecosystems 17: 673-684.

Wang M, Moore TR, Talbot J, Riley JL. 2015. The stoichiometry of carbon and nutrients in peat formation. Global Biogeochemical Cycles 29: 113-121.

Wang M, Talbot J, Moore TR. 2018. Drainage and fertilization effects on nutrient availability in an ombrotrophic peatland. Science of the Total Environment 621: 1255-1263.

Weedon JT, Kowalchuk GA, Aerts R, van Hal J, van Logtestijn R, Taş N, Röling WFM, van Bodegom PM. 2012. Summer warming accelerates sub-arctic peatland nitrogen cycling without changing enzyme pools or microbial community structure. Global Change Biology 18: 138-150.

Weltzin JF, Bridgham SD, Pastor J, Chen J, Harth C. 2003. Potential effects of warming and drying on peatland plant community composition. Global Change Biology 9: 141-151.

Wilson RM, Griffiths NA, Visser A, McFarlane KJ, Sebestyen SD, Oleheiser KC, Bosman S, Hopple AM, Tfaily MM, Kolka RK, Hanson PJ, Kostka JE, Bridgham SD, Keller JK, Chanton JP. 2021a. Radiocarbon analyses quantify peat carbon losses with increasing temperature in a whole ecosystem warming experiment, Journal of Geophysical Research: Biogeosciences 126: e2021JG006511.

Wilson RM, Tfaily MM, Kolton M, Johnston ER, Petro C, Zalman CA, Hanson PJ, Heyman HM, Kyle JE, Hoyt DW, Eder EK, Purvine SO, Kolka RK, Sebestyen SD, Griffiths NA, Schadt CW, Keller JK, Bridgham SD, Chanton JP, Kostka JE. 2021b. Soil metabolome response to whole-ecosystem warming at the Spruce and Peatland Responses under Changing Environments experiment, Proceedings of the National Academy of Sciences 118: e2004192118.

Yang JE, Skogley EO, Georgitis SJ, Schaff BE, Ferguson AH. 1991. Phytoavailability soil test: Development and verification of theory. Soil Science Society of America Journal 55: 1358-1365.

Yang X, Ricciuto DM, Thornton PE, Shi X, Xu M, Hoffman F, Norby RJ. 2019. The effects of phosphorus cycle dynamics on carbon sources and sinks in the Amazon region: A modeling study using ELM v1. Journal of Geophysical Research: Biogeosciences 124: 3686-3698.

Supporting information

The supporting information is incorporated into one document that includes: (1) *Supplementary Statistical Methods*, including linear, mixed-effects model selection for both annual and monthly models, as well as (2) Supplementary Tables (Tables S1 – S5), and (3) Supplementary Figures (Figures S1 – S7).

Tables

Table 1. Cumulative annual resin-available NH_4-N and PO_4-P, and their annual ratio, across experimental treatments, microtopographic positions, and peat depths from 2014 to 2018.

Year	Atmospheric [CO_2]	Micro-topography	Depth (cm)	Cumulative annual available NH_4-N ($\mu g\ N\ cm^{-2}\ year^{-1}$)						Cumulative annual available PO_4-P ($\mu g\ P\ cm^{-2}\ year^{-1}$)						Cumulative annual N/P ratio					
				Amb.	0°C	2.25°C	4.5°C	6.75°C	9°C	Amb.	0°C	2.25°C	4.5°C	6.75°C	9°C	Amb.	0°C	2.25° C	4.5°C	6.75° C	9°C
2014	Ambient	Hummock	10	6 ± 2	12	15	11	7	15	1.0 ± 1.3	0.7	3.5	1.3	0.6	2.3	31 ± 12	113	4	67	26	8
			30	38 ± 17	11	35	20	13	18	6.1 ± 2.8	1.3	3.2	6.1	4.3	2.3	7 ± 0	8	25	3	4	8
			60	115 ± 51	25	140	143	152	90	10.8 ± 1.3	3.9	9.3	25.0	24.1	15.4	11 ± 6	7	17	5	8	6
		Hollow	10	20 ± 8	20	23	13	13	31	3.3 ± 1.0	1.9	6.9	3.0	3.1	6.6	6 ± 1	11	3	4	44	5
			30	24 ± 14	12	84	49	26	32	2.8 ± 2.8	1.7	13.1	9.1	3.9	4.6	37 ± 42	8	6	6	6	7
	Elevated	Hummock	10	--	11	10	11	4	4	--	3.3	0.1	1.3	2.6	0.2	--	8	175	52	2	28
			30	--	17	21	23	43	17	--	3.3	2.5	5.0	12.2	2.2	--	5	10	6	4	105
			60	--	115	49	31	347	33	--	25.3	7.9	4.7	56.1	9.8	--	5	6	8	6	6
		Hollow	10	--	26	13	29	56	18	--	5.5	6.9	4.6	10.7	1.9	--	5	3	6	4	83
			30	--	77	33	28	179	37	--	7.0	2.6	2.7	36.1	5.9	--	11	13	39	5	7
2015	Ambient	Hummock	10	7 ± 4	6	7	10	11	17	1.5 ± 1.2	1.3	0.9	1.4	3.3	3.2	5 ± 1	5	7	8	3	6
			30	25 ± 6	10	23	15	16	16	1.6 ± 0.0	1.1	0.9	3.4	9.0	2.2	16 ± 4	9	27	4	2	9
			60	73 ± 24	16	178	106	174	116	3.0 ± 1.7	1.4	10.1	8.7	4.6	4.3	33 ± 29	11	23	10	41	25
		Hollow	10	16 ± 9	18	13	14	20	28	1.5 ± 0.7	5.3	0.9	2.3	11.0	5.4	11 ± 2	4	14	6	2	5
			30	17 ± 4	10	70	32	42	69	1.8 ± 1.3	1.1	1.9	4.7	3.4	3.5	12 ± 5	9	38	6	12	19
	Elevated	Hummock	10	--	1	7	7	5	15	--	0.6	0.7	2.2	1.4	2.2	--	2	9	5	4	7
			30	--	21	16	11	32	20	--	1.1	1.3	1.9	6.6	3.0	--	19	13	7	5	6
			60	--	50	35	27	407	59	--	3.7	2.1	2.3	54.1	4.5	--	13	14	12	9	13
		Hollow	10	--	19	17	11	77	24	--	4.5	2.5	1.8	31.2	4.2	--	8	7	6	2	6
			30	--	27	23	26	227	34	--	2.6	1.7	2.6	32.5	3.2	--	10	15	8	9	11
2016	Ambient	Hummock	10	3 ± 0	8	13	5	2	20	0.4 ± 0.1	1.1	1.9	0.7	2.3	4.4	13 ± 2	9	7	11	1	5
			30	22 ± 3	22	31	37	42	31	1.1 ± 0.1	2.9	4.3	6.5	29.3	4.7	24 ± 12	12	15	6	2	8
			60	78 ± 30	16	157	170	209	173	1.9 ± 0.1	0.7	11.2	15.3	12.1	16.0	41 ± 11	43	16	16	28	14
		Hollow	10	16 ± 5	23	27	12	11	33	1.1 ± 0.2	11.1	4.1	1.9	9.1	4.0	21 ± 9	3	7	8	4	9
			30	17 ± 6	9	78	52	100	122	0.8 ± 0.2	1.2	7.8	8.5	8.8	13.9	44 ± 32	7	13	7	10	8
	Elevated	Hummock	10	--	8	6	4	4	9	--	1.7	0.7	1.4	1.7	1.8	--	24	9	3	6	10
			30	--	15	7	63	99	17	--	3.0	1.3	6.8	20.7	2.9	--	5	9	9	5	6
			60	--	30	19	54	492	165	--	3.2	1.9	2.5	46.0	15.4	--	9	9	20	11	11
		Hollow	10	--	38	18	44	207	8	--	11.4	2.8	3.9	33.4	4.4	--	3	6	11	5	3
			30	--	25	30	44	428	97	--	5.8	7.1	3.0	40.3	7.4	--	5	4	16	10	14
2017	Ambient	Hummock	10	8 ± 5	2	5	10	7	10	1.0 ± 0.7	0.3	0.6	1.7	6.0	2.9	9 ± 2	8	7	6	6	3
			30	14 ± 2	23	20	98	19	34	1.0 ± 0.3	1.4	1.9	22.7	4.6	2.2	31 ± 9	17	18	6	18	22
			60	66 ± 21	17	156	217	273	288	1.4 ± 0.0	0.5	9.7	21.0	14.4	41.8	110 ± 99	42	42	17	30	16
		Hollow	10	14 ± 4	9	16	20	14	25	0.7 ± 0.0	1.1	1.5	2.6	6.9	7.8	22 ± 5	23	11	8	18	4
			30	15 ± 4	9	64	75	127	136	0.5 ± 0.2	0.5	7.1	11.8	4.8	17.7	37 ± 15	19	13	16	20	12
	Elevated	Hummock	10	--	3	6	8	8	9	--	0.5	0.8	2.7	1.8	1.3	--	8	8	3	9	11
			30	--	30	10	31	142	49	--	7.7	0.8	2.1	23.1	5.2	--	4	11	16	6	10
			60	--	23	20	85	577	281	--	2.5	2.1	4.9	60.3	23.6	--	36	8	14	9	12
		Hollow	10	--	22	13	25	191	7	--	7.6	2.1	2.3	33.1	0.6	--	3	10	10	5	15
			30	--	20	20	33	484	110	--	5.9	2.7	1.5	47.5	4.8	--	5	8	20	10	23

2018	Ambient	Hummock	10	6 ± 3	6	13	16	69	330	1.4 ± 0.8	0.7	6.0	9.1	34.7	78.0	6 ± 0	9	2	2	2	4
			30	13 ± 0	17	21	35	85	259	1.8 ± 1.8	0.7	8.3	9.8	41.5	30.0	16 ± 16	28	3	4	3	8
			60	63 ± 33	19	159	181	290	409	2.9 ± 2.3	0.6	14.0	14.6	18.0	42.7	24 ± 8	31	13	15	32	14
		Hollow	10	18 ± 0	9	39	16	108	414	2.1 ± 1.3	2.7	10.7	5.3	33.5	75.6	11 ± 6	3	5	5	3	6
			30	9 ± 3	6	118	67	152	501	1.7 ± 0.1	0.6	5.4	9.9	14.7	73.2	9 ± 4	10	21	8	16	7
	Elevated	Hummock	10	--	6	6	61	23	14	--	10.3	0.8	25.1	33.4	3.2	--	1	8	2	1	3
			30	--	45	10	49	243	36	--	16.5	1.8	6.7	51.3	5.3	--	3	5	8	5	7
			60	--	44	21	109	501	286	--	8.8	1.8	4.6	72.9	13.9	--	5	11	19	7	22
		Hollow	10	--	19	28	113	367	14	--	17.0	14.9	20.0	85.9	2.2	--	1	2	7	4	7
			30	--	35	24	53	411	104	--	17.0	8.4	7.6	66.9	2.9	--	2	4	12	7	34

Notes: We sampled the SPRUCE experimental plots in 2013, but do not include the annual totals here. We sampled only three months in the summer, directly after installation in June 2013, and we expected some disturbance associated with access-tube installation along with a shortened collection timeframe that precluded a full assessment of annual nutrient accumulation. Note that 'cm^2' was the surface area of the half of the resin capsule that was in contact with the surrounding peat (i.e., Figure S1f). Where an 'A' or 'B' sub-replicate sample was (rarely) missing or lost at a given sampling date, we inserted the value for the other sub-replicate in order to calculate an annual sum; data for each year, depth, and topographic position are averaged across the annual accumulated resin-available nutrients at the A and B location in each enclosure. Note that the NH_4-N and PO_4-P cumulative annual data can also be found in Figure 3, but given the wide range across orders of magnitude of the data, we also include the data here. We also include the data from the ambient plots (i.e., 'Amb.', plots without an enclosure that receive no warming or elevated [CO_2]); ambient data for each year, depth, and topographic position are averaged across the annual accumulated resin-available nutrients at the A and B location in each of two ambient plots, which were then averaged ± 1 SD.

Figures

Figure 1 A pictogram of the layout of the SPRUCE experimental enclosures and their associated treatments. The SPRUCE experimental enclosures were warmed above- and belowground in a regression design spanning +0°C to +9°C; half of the enclosures also received +500 ppm CO_2 (highlighted in this pictogram with green octagons). There are also two fully-instrumented ambient reference plots without enclosures. Resin-access tubes were installed at multiple depths at two locations (A and B) in each enclosure or ambient plot in paired hummock-hollow microtopography at each location (see inset diagram). SPRUCE site pictogram courtesy of Brett Hopwood, ORNL Graphics, as in Seay (2018).

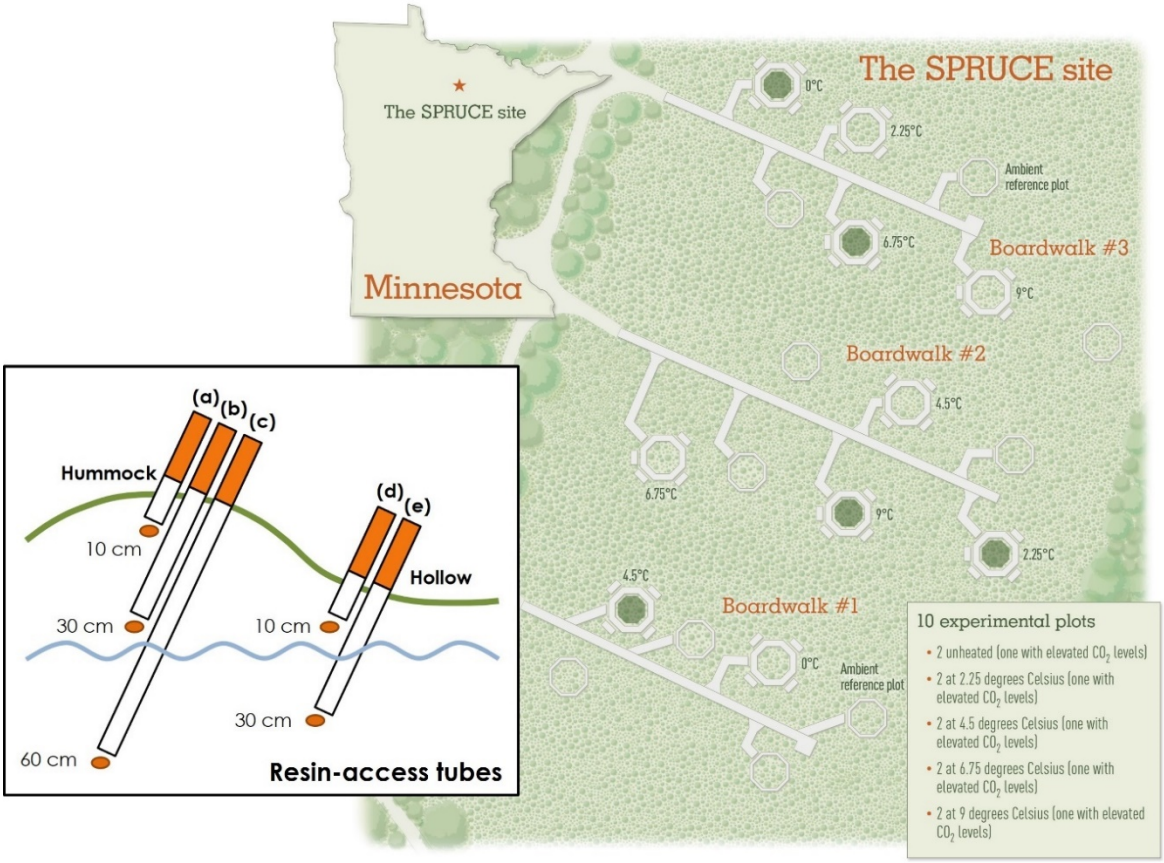

Figure 2 Linear mixed-effects model beta coefficients and their 95% confidence intervals. The coefficients correspond to the factors in the final linear mixed-effect models for the effects of warming, microtopography and depth (as 'topodepth', which treats each microtopographic position and depth as discrete locations), and year, and the interactive effects of warming × topodepth and warming × year on resin-available NH_4-N, PO_4-P and the ratio of NH_4-N to PO_4-P (see *Supplementary Statistical Methods* for selection of final models). The beta coefficients for warming, year, and topodepth were added for reference but cannot be interpreted in isolation because of significant interactions. For each factor and interaction, the beta coefficients represent the difference between a baseline (alphabetically or numerically the first level) and the other levels of each factor or interactions. For example, for years, the baseline is the year 2014 and for topodepth, the baseline is Ho10 ('hollow, 10 cm peat depth'). The final model was different for the N/P ratio, as it included an additional topodepth × year interaction term; the full range of beta coefficients for all of the interactions in the N/P ratio model are included in Figure S2. Asterisks indicate level of significance at $P < 0.001$***; $P < 0.01$** and $P < 0.05$*.

Figure 2

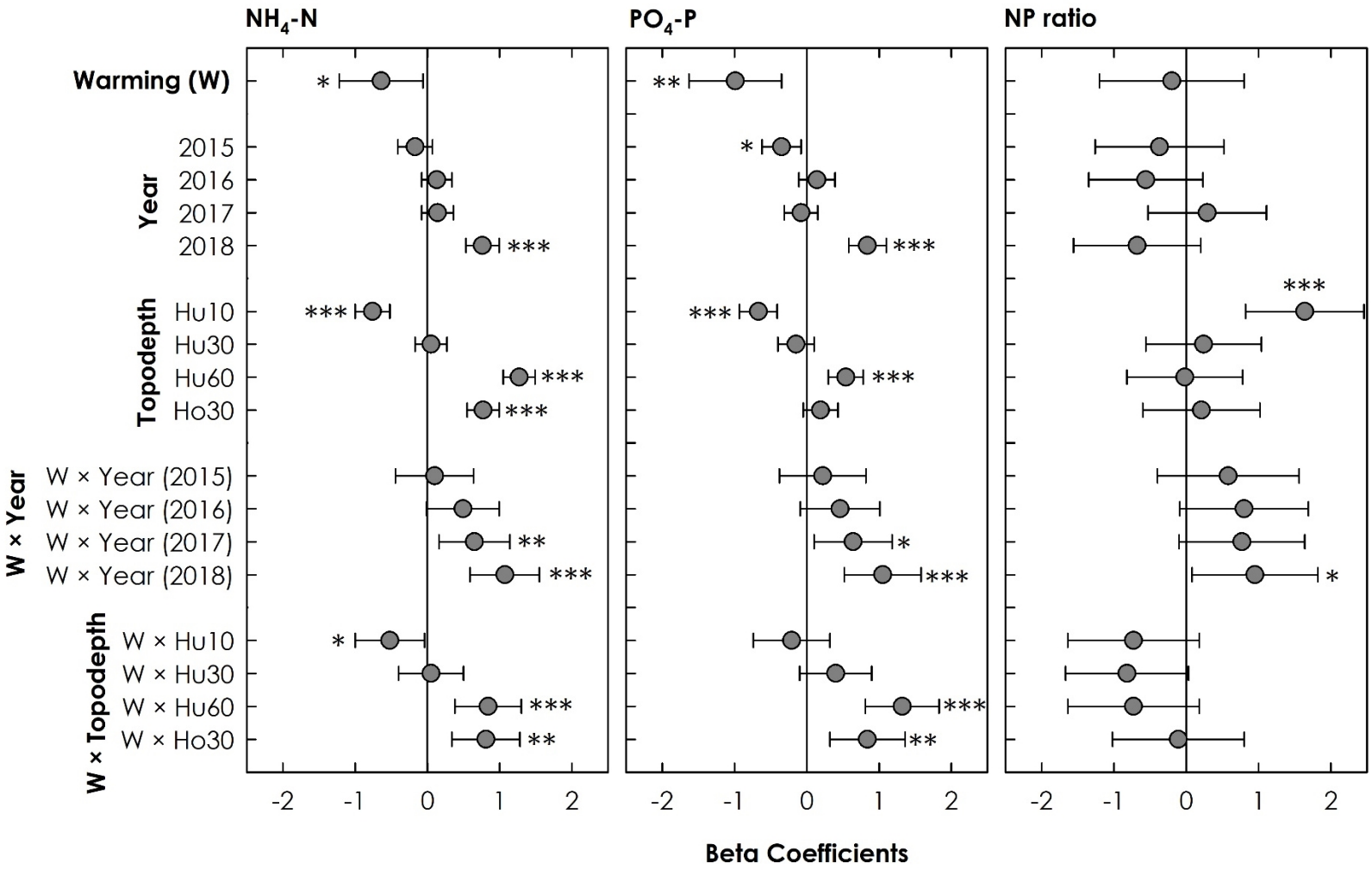
NH4-N
PO4-P
NP ratio
Warming (W)
Year
2015
2016
2017
2018
Topodepth
Hu10
Hu30
Hu60
Ho30
W × Year
W × Year (2015)
W × Year (2016)
W × Year (2017)
W × Year (2018)
W × Topodepth
W × Hu10
W × Hu30
W × Hu60
W × Ho30
-2
-1
0
1
2
Beta Coefficients

Figure 3 Annual, cumulative NH_4-N or PO_4-P adsorbed to ion-exchange resins regressed against annual average peat temperature at a depth closest to the depth of resin incubation. The panels represent multiple peat depths in hummock and hollow microtopography, and the observations span a gradient of whole-ecosystem warming and warming combined with elevated [CO_2]. Each data point is one enclosure, in years 2014 to 2018. Closed symbols are ambient [CO_2] while open symbols are elevated [CO_2]; all data shown were included in log-linear regressions. More intense colors correspond with more recent years. The full range of colors and symbols are listed here; henceforth figure legends include colors for 2018 only. Letter insets correspond to depth of resin incubation (a, b, and c are 10, 30, and 60-cm depths in hummocks and d and e are 10 and 30-cm depths in hollows, respectively, see inset in Figure 1). Asterisks indicate level of significance corresponding to log-linear regression at $P < 0.001$***; $P < 0.01$** and $P < 0.05$*, and R^2 is the adjusted R^2 of NH_4-N regression (upper right of each panel) or PO_4-P regression (lower right of each panel); note the log-scale of the y-axis. See Table S4 for regression parameters (predicted resin-available nutrients were back-transformed for the purposes of the lines presented in this figure).

Figure 3

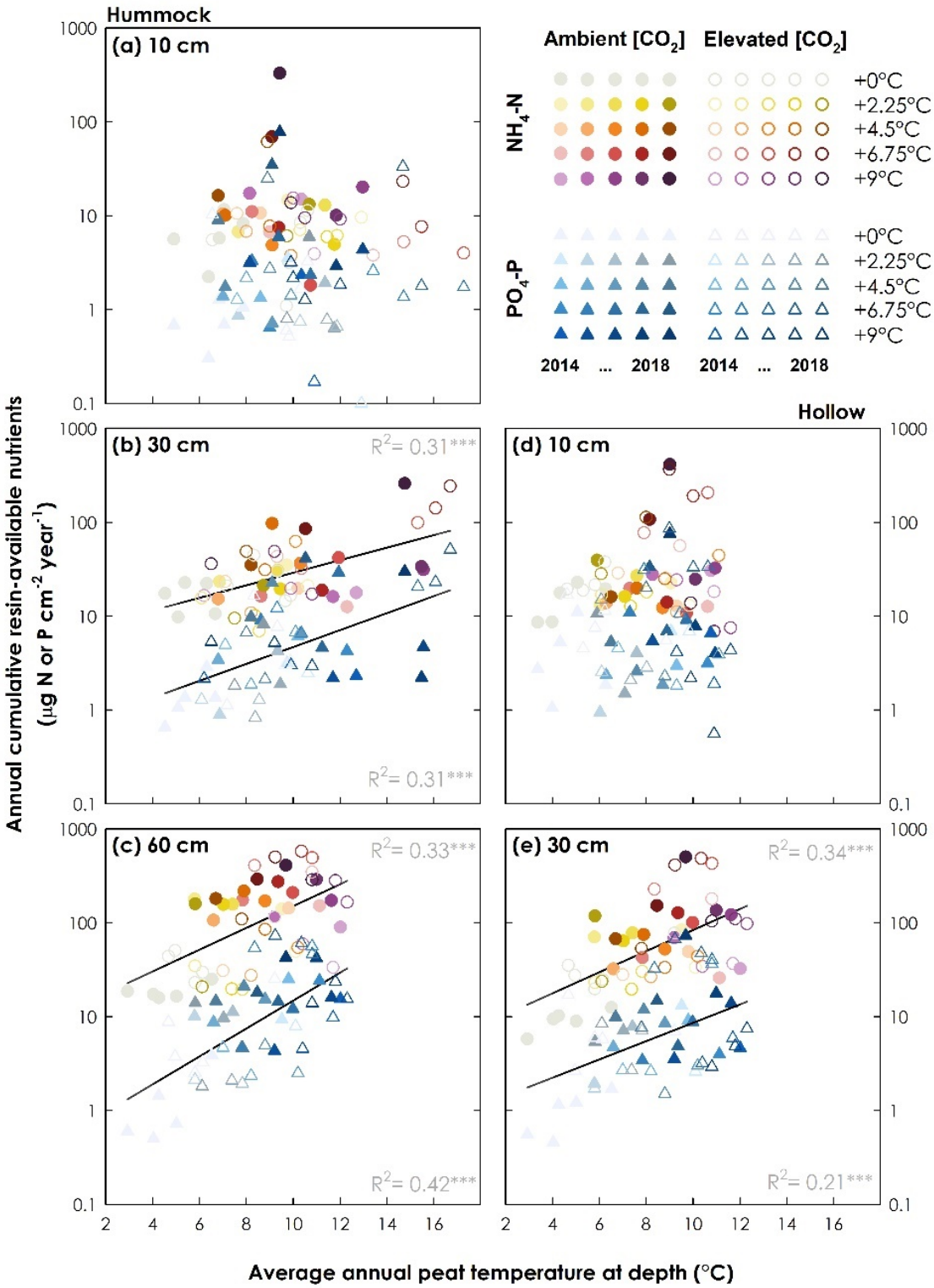
Hummock
Hollow
(a) 10 cm
(b) 30 cm
(c) 60 cm
(d) 10 cm
(e) 30 cm
Ambient [CO2]
Elevated [CO2]
NH4-N
PO4-P
+0°C
+2.25°C
+4.5°C
+6.75°C
+9°C
2014 ... 2018 2014 ... 2018
R2= 0.31***
R2= 0.31***
R2= 0.33***
R2= 0.42***
R2= 0.34***
R2= 0.21***
Annual cumulative resin-available nutrients (μg N or P cm-2 year-1)
Average annual peat temperature at depth (°C)

Figure 4 ELM-SPRUCE model prediction of net N mineralization and net P mineralization (inset). Each data point is one SPRUCE enclosure, in years 2016 to 2018. More intense colors correspond with more recent years (see full year-color array in Figure 3); closed symbols are ambient [CO_2] while open symbols are elevated [CO_2]. Letter insets correspond to depth of resin incubation (a, b, and c are 10, 30, and 60-cm depths in hummocks and d and e are 10 and 30-cm depths in hollows, see inset in Figure 1). Note that model output data are in units of g nutrient per unit soil volume per year; also note the differences in the y-axis for the net P mineralization figures, as model-predicted net P mineralization was quite low at some peat depths.

Figure 4

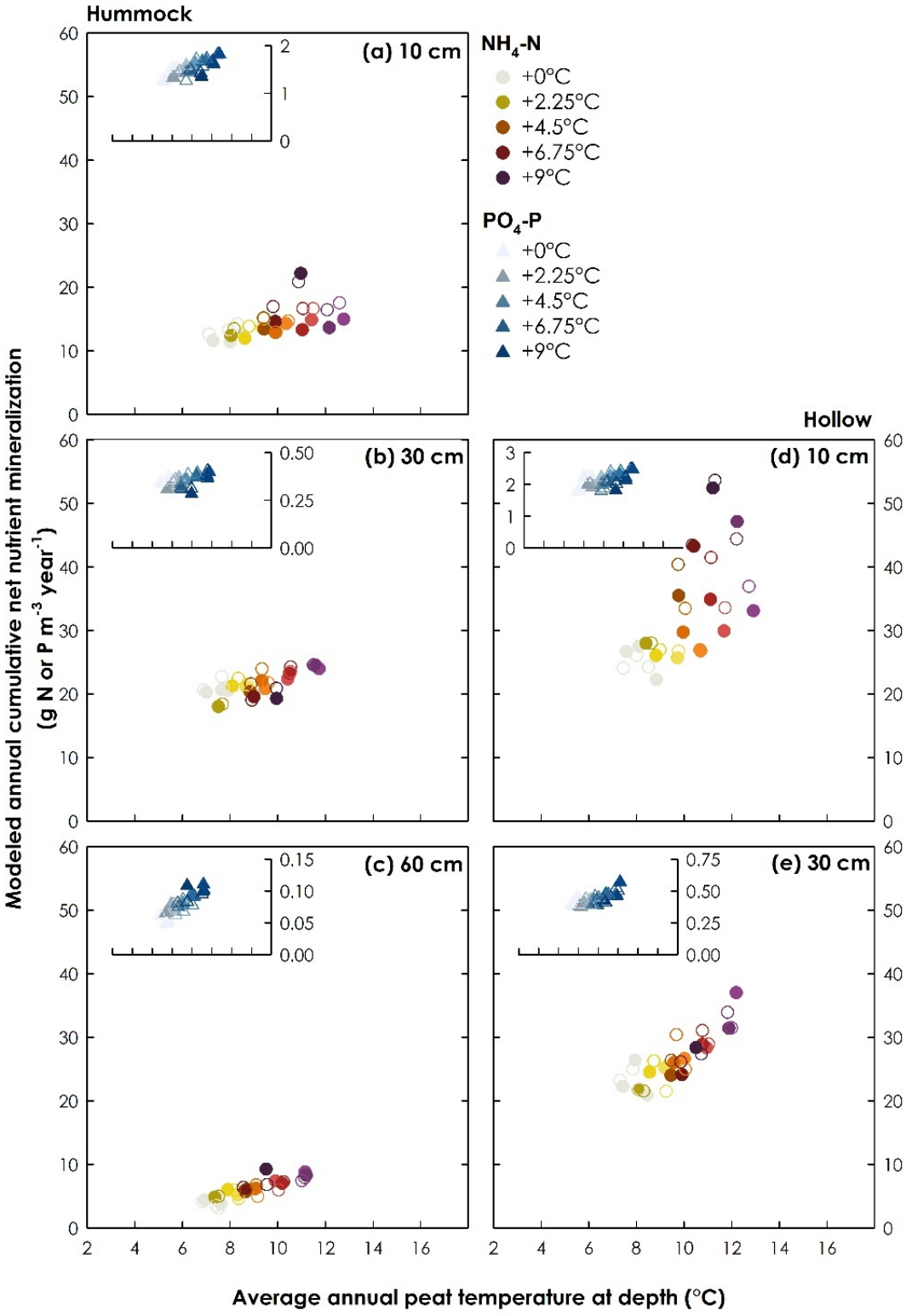
Hummock
Hollow
(a) 10 cm
(b) 30 cm
(c) 60 cm
(d) 10 cm
(e) 30 cm
NH4-N
+0°C
+2.25°C
+4.5°C
+6.75°C
+9°C
PO4-P
+0°C
+2.25°C
+4.5°C
+6.75°C
+9°C
Modeled annual cumulative net nutrient mineralization (g N or P m-3 year-1)
Average annual peat temperature at depth (°C)

Figure 5 Relationship between *Sphagnum* moss N and P requirements and annual cumulative resin-available NH_4-N and PO_4-P. Declining *Sphagnum* N and P requirement with warming from 2016 to 2018 (see Figure S3) could have been a causal factor in the large increases in resin-available NH_4-N and PO_4-P at 10-cm peat depth in more recent years in both hummocks and hollows (hummock microtopography is designated with black circle outline in both panels; note differences in y-axes between NH_4-N and PO_4-P). Cumulative annual nutrient predictions were back-transformed to fit to data on graph; R^2 shown are adjusted R^2. More intense colors represent more recent years (see full year-color array in Figure 3); closed symbols are ambient [CO_2] while open symbols are elevated [CO_2]. Note that the x-axis is plotted from greatest to least *Sphagnum* N and P requirement to highlight the relationship between declining *Sphagnum* nutrient requirement and increasing resin-available N and P. The log-linear relationships between log-transformed cumulative annual NH_4-N and PO_4-P and *Sphagnum* N or P requirement over the years 2016 – 2018 were as follows: $\log_{10}(NH_4\text{-N}) = -0.32^{***} (\pm 0.07\ SE) \times Sphagnum\ N_{req} + 1.56^{***} (\pm 0.10\ SE)$ and $\log_{10}(PO_4\text{-P}) = -2.46^{*} (\pm 1.04\ SE) \times Sphagnum\ P_{req} + 0.86^{***} (\pm 0.14\ SE)$, respectively (asterisks indicate level of significance for intercept and slope, where * is $P < 0.05$ and *** is $P < 0.0001$).

Figure 5

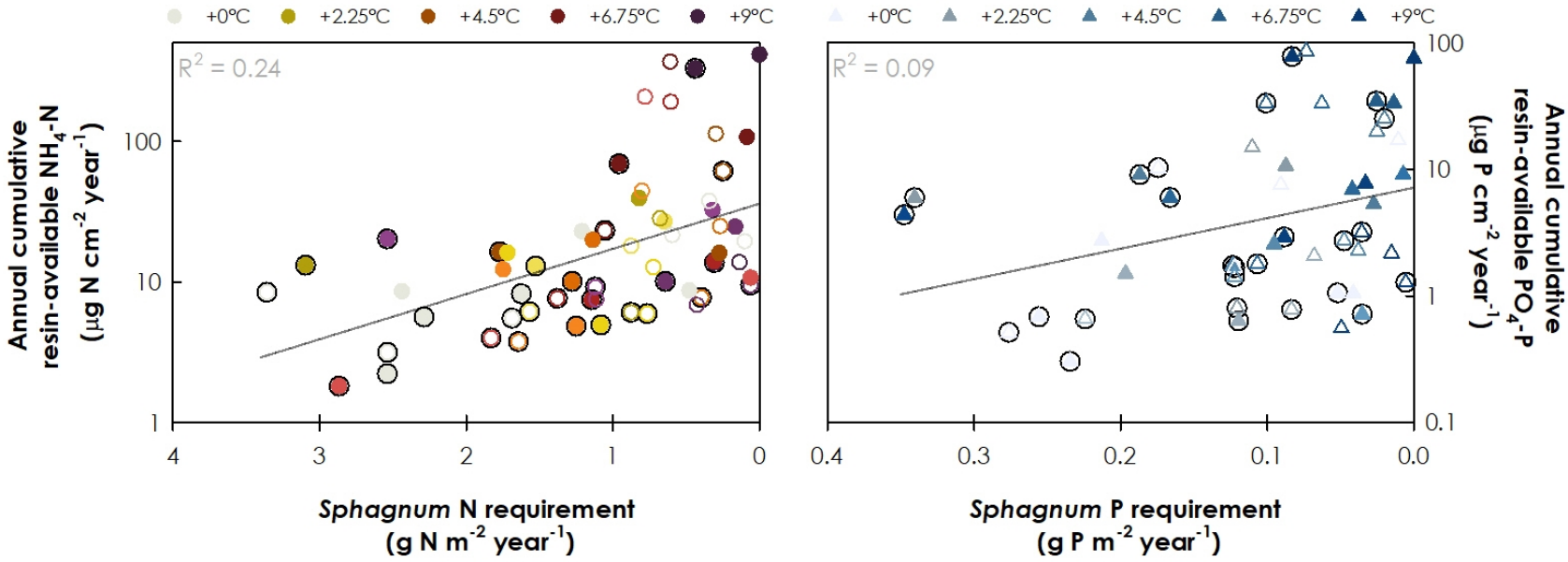
+0°C
+2.25°C
+4.5°C
+6.75°C
+9°C
R² = 0.24
Annual cumulative resin-available NH4-N (µg N cm-2 year-1)
100
10
1
4
3
2
1
0
Sphagnum N requirement (g N m-2 year-1)
R² = 0.09
Annual cumulative resin-available PO4-P (µg P cm-2 year-1)
100
10
1
0.1
0.4
0.3
0.2
0.1
0.0
Sphagnum P requirement (g P m-2 year-1)

Figure 6 Temperature response functions for NH_4-N for approximately 28-day resin collections in 2018. Grey text indicates parameters from a significant Q_{10} response function ± 1 SE ($P \leq 0.05$), where R_{12} is the baseline amount of NH_4-N available at 12°C ± 1 SE, *n* is the number of observations from monthly NH_4-N accumulation on resins sampled for ~28 days across all enclosures over 9 sampling periods in 2018 for A and B subplots within each enclosure, and R^2 is the adjusted R^2. Peat temperature at depth was the average temperature at the depth at which the resin was incubated (see Table S2) during the incubation period. PO_4-P data from 2018 only are in Figure S4 and all resin-available nutrient data for both NH_4-N and PO_4-P from 2014 to 2018 are in Figures S5 and S6, respectively, and have been appended to Iversen and others (2017, data citation). Closed symbols are ambient [CO_2] while open symbols are elevated [CO_2]. Letter insets correspond to depth of resin incubation (a, b, and c are 10, 30, and 60-cm depths in hummocks and d and e are 10 and 30-cm depths in hollows, see inset in Figure 1).

Figure 6

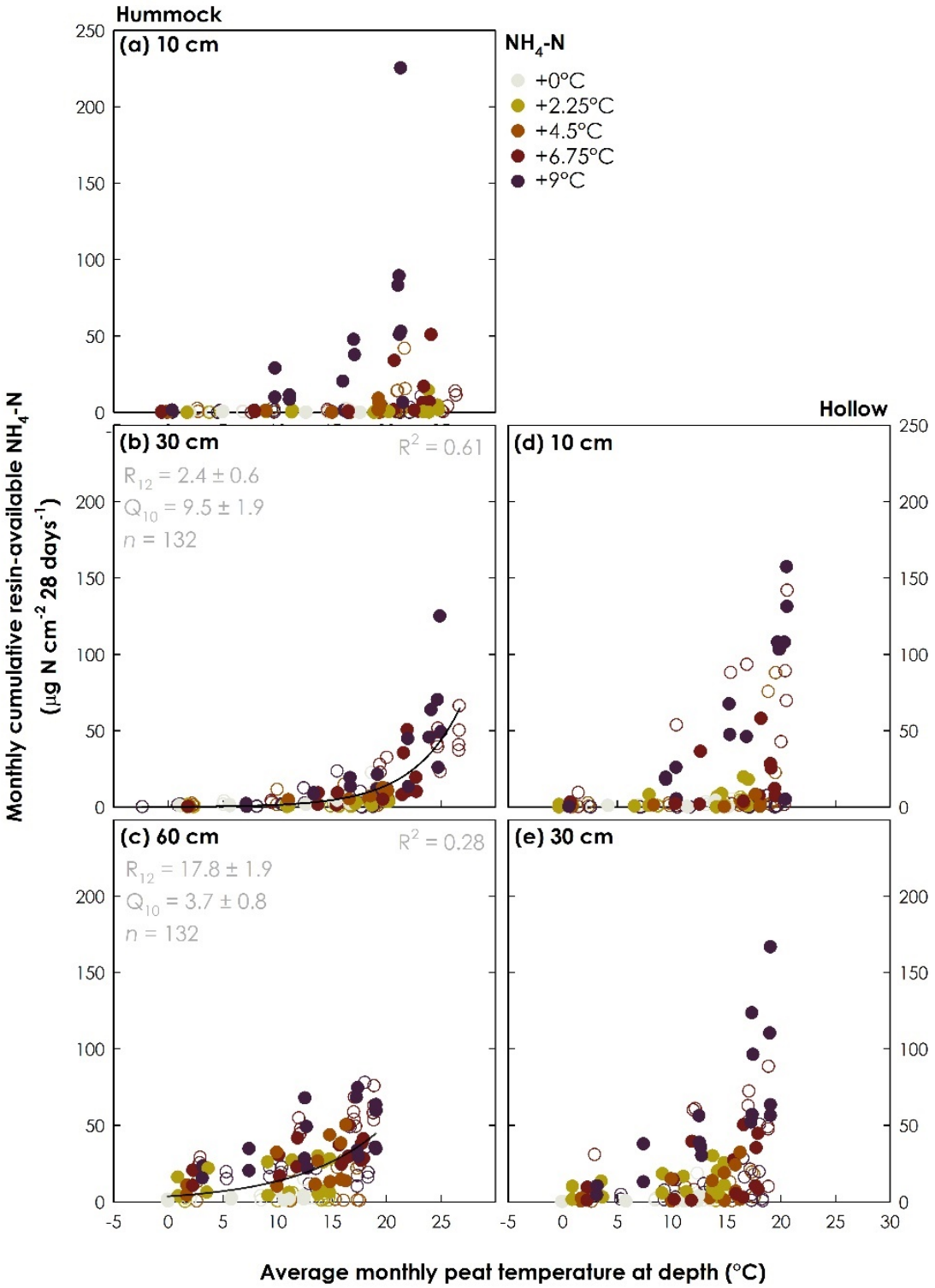
Hummock
Hollow
(a) 10 cm
(b) 30 cm
(c) 60 cm
(d) 10 cm
(e) 30 cm
NH4-N
+0°C
+2.25°C
+4.5°C
+6.75°C
+9°C
R2 = 0.61
R12 = 2.4 ± 0.6
Q10 = 9.5 ± 1.9
n = 132
R2 = 0.28
R12 = 17.8 ± 1.9
Q10 = 3.7 ± 0.8
n = 132
Monthly cumulative resin-available NH4-N (μg N cm-2 28 days-1)
Average monthly peat temperature at depth (°C)

Figure 7. The relationship between resin-available PO_4-P and NH_4-N (i.e., the N/P ratio) across SPRUCE experimental treatments. The data span all enclosures, sub-replicates, peat depths, and sampling dates from 2014 to 2018, standardized to a 28-day sampling interval; the dashed lines are the 1:1 line. Given the log scale, any NH_4-N and PO_4-P observations that were determined to be '0' after blank correction are not shown. More intense colors represent more recent years (see full year-color array in Figure 3); closed symbols are ambient [CO_2] while open symbols are elevated [CO_2] (note that the color scheme has been used previously for NH_4-N data only, but we also use here for the N/P ratio to avoid introducing yet another color array). Letter insets correspond to depth of resin incubation (a, b, and c are 10, 30, and 60-cm depths in hummocks and d and e are 10 and 30-cm depths in hollows, respectively, see inset in Figure 1).

Figure 7

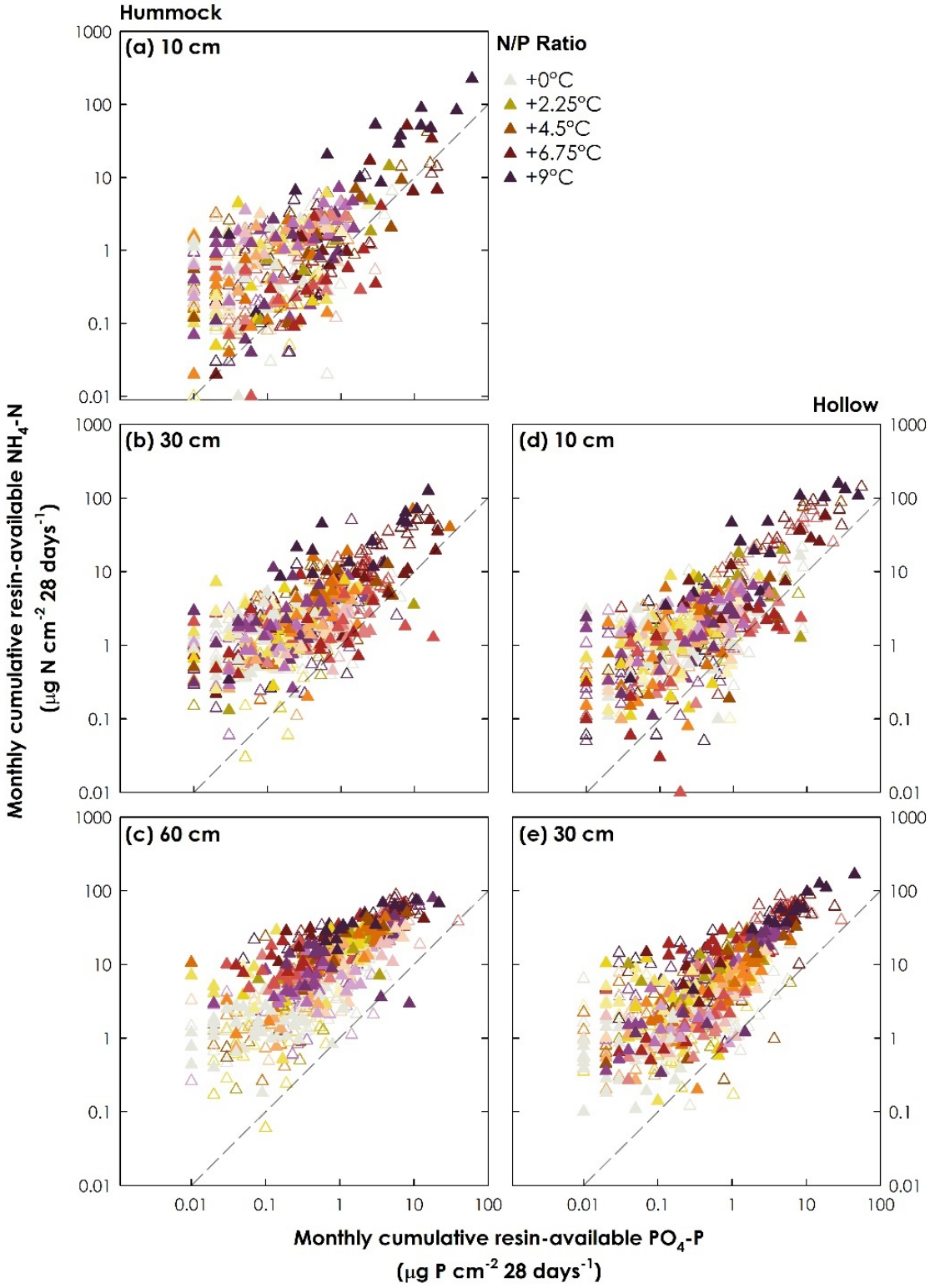
Hummock
Hollow
(a) 10 cm
(b) 30 cm
(c) 60 cm
(d) 10 cm
(e) 30 cm
N/P Ratio
+0°C
+2.25°C
+4.5°C
+6.75°C
+9°C
Monthly cumulative resin-available NH4-N
(µg N cm-2 28 days-1)
Monthly cumulative resin-available PO4-P
(µg P cm-2 28 days-1)
0.01
0.1
1
10
100
1000

Figure 8. Comparisons of resin-available NH_4-N with inorganic, organic, and total N concentrations in porewater. Data span 2015 – 2018, at 10 cm or 30 cm depth in the hollows only, and nutrient data from discrete ~biweekly porewater collections were averaged within the dates of the ~monthly resin incubations. More intense colors represent more recent years (see full year-color array in Figure 3); closed symbols are ambient [CO_2] while open symbols are elevated [CO_2]. For the purposes of this analysis, we focused on the porewater nutrient concentrations at 0-10 cm and 30-40 cm piezometer depths to facilitate direct comparison with ion-exchange resins incubated at those depths in adjacent hollows (i.e., from only one, adjacent resin array per enclosure). Note that the units for porewater nutrients are g nutrient per L of porewater, while the units for resin-available nutrients have been standardized to the resin surface area. Comparisons of resin-available PO_4-P with porewater P concentrations are in Figure S7.

Figure 8

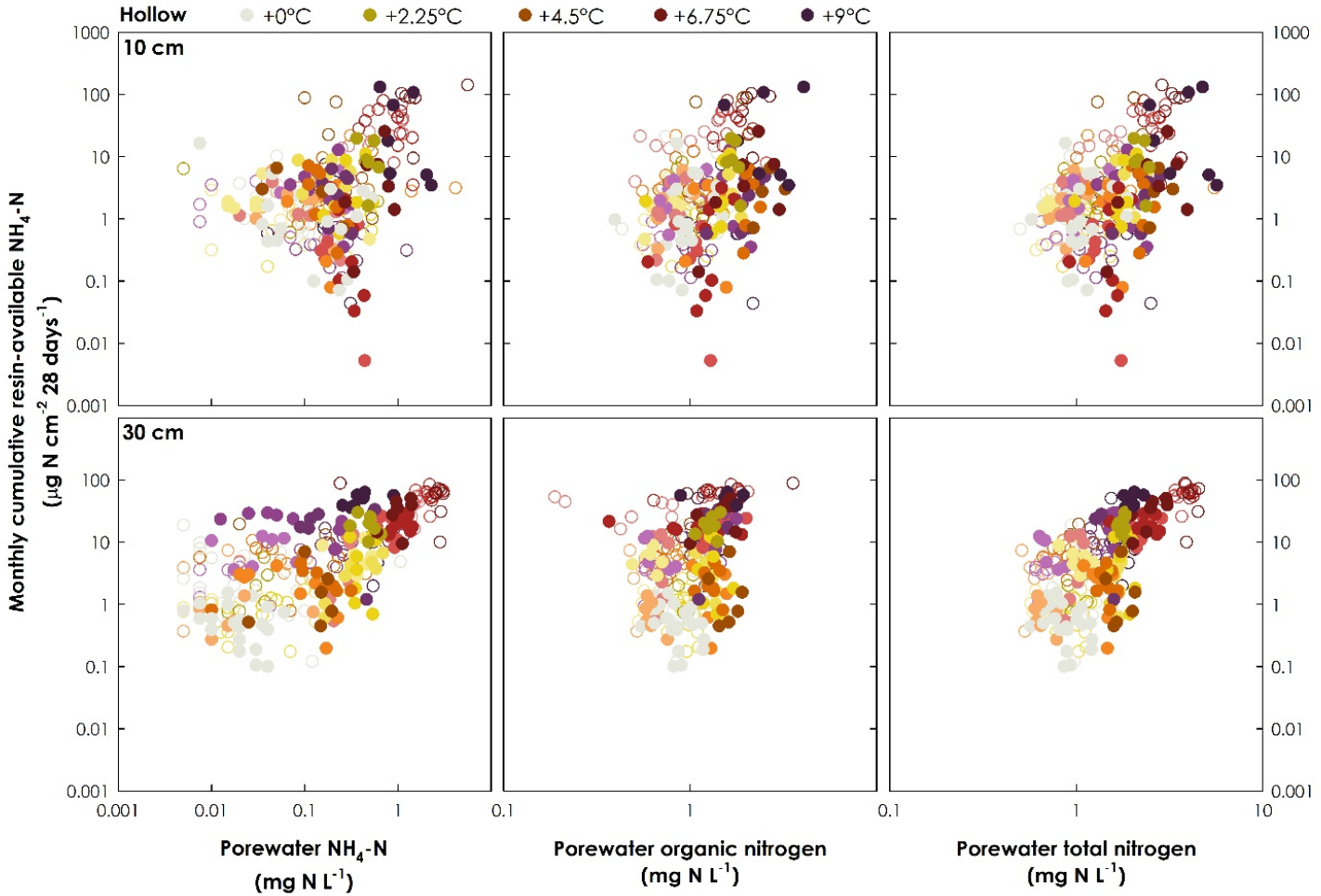
Hollow
+0°C
+2.25°C
+4.5°C
+6.75°C
+9°C
10 cm
30 cm
Monthly cumulative resin-available NH4-N
(μg N cm-2 28 days-1)
Porewater NH4-N
(mg N L-1)
Porewater organic nitrogen
(mg N L-1)
Porewater total nitrogen
(mg N L-1)